Please cite this article in press as: Xia et al., Practical Challenges and Future Perspectives of All-Solid-State Lithium-Metal Batteries, Chem (2018), https://doi.org/10.1016/j.chempr.2018.11.013

Chem

CellPress
REVIEWS

Review

Practical Challenges and Future Perspectives of All-Solid-State Lithium-Metal Batteries

Shuixin Xia,[1,4] Xinsheng Wu,[1,4] Zhichu Zhang,[1] Yi Cui,[2,3,*] and Wei Liu[1,*]

The fundamental understandings and technological innovations in lithium-ion batteries are essential for delivering high energy density, stable cyclability, and cost-effective energy storages with the growing demands in the applications of electrical vehicles and smart grid. Solid-state electrolytes (SSEs) are more promising than organic liquid electrolyte in terms of excellent safety in developing lithium-metal anode as well as other high-capacity cathode chemistries, such as sulfur and oxygen. Considerable efforts have been made to give birth to the superionic conductors with ionic conductivities higher than 10^{-3} S cm^{-1} at room temperature. However, the high interfacial impedances from the poor compatibility of SSEs with electrodes limit their practical applications, which are discussed in this review. Furthermore, the recent advances and critical challenges for all-solid-state lithium-metal batteries based on the cathode materials of lithium-intercalation compounds, sulfur, and oxygen are overviewed, and their future developments are also prospected.

INTRODUCTION

The tremendous depletion of fossil energy and the ever-increasing demand in sustainable energy have spurred the research for low-cost, environmentally friendly, and high-performance energy conversion and storage systems. Particularly, lithium (Li)-ion batteries (LIBs) are one of the most promising energy-storage candidates for their high energy density, superior cycling stability, and light weight. The evolution of LIBs has undergone a progress from Li-metal batteries (LMBs) based on Li-metal anode to LIBs using Li-intercalation compound electrode, and then to the revival of LMBs (Figure 1). The earliest LMBs can be traced back to 1980 when Moli Energy developed Li-MoS_2 batteries with liquid electrolyte.[1] Unfortunately, the use of Li-metal anode is prone to cause safety concerns resulting from the dendrite growth that could penetrate the separator and lead to cell short-circuit and even cause fire.[2] By replacing Li metal with carbonaceous anode, Sony firstly fabricated the earliest commercial LIBs with improved safety in 1990 using $LiCoO_2$ (LCO) cathode with liquid electrolyte of $LiPF_6$ in propylene carbonate and ethylene carbonate.[3] In the past two decades, state-of-the-art LIBs, with an achievable energy density of ~250 Wh kg^{-1},[4] still could not satisfy the increasing demand for higher energy density in the applications of large-scale energy storage. In addition, the frequently used organic liquid electrolytes with properties such as flammability, corrosivity, and thermal instability for LIBs can cause serious safety issues, blocking their wide applications. As a result, new approaches including advanced separators,[5] electrolyte additives,[6] and positive temperature coefficient (PTC)-modified current collectors[7] have been proposed to improve safety. Hence, new chemistries or technologies for Li-based batteries with higher energy density, longer cycle life, and higher safety are being urgently developed.

The Bigger Picture

Lithium-ion batteries are one of the most promising energy-storage devices for their high energy density, superior cycling stability, and light weight. However, the state-of-the-art lithium-ion batteries cannot satisfy the rising demand of high energy density. Advanced lithium batteries based on metallic lithium anodes could provide higher energy density and thus become a hot research topic. The main challenges of developing lithium-metal anodes are the dendritic growth with a possibility of short circuit (leading to thermal runaway) and the low Coulombic efficiency with poor cycle life. Developing lithium-metal batteries based on solid electrolytes can fundamentally alleviate the safety concerns. This review highlights the most recent approaches to addressing the sluggish ion transport of solid-state electrolyte as well as the high impedances at the electrode-electrolyte interface. The critical challenges and future developments for all-solid-state lithium-metal batteries are also discussed.

Please cite this article in press as: Xia et al., Practical Challenges and Future Perspectives of All-Solid-State Lithium-Metal Batteries, Chem (2018), https://doi.org/10.1016/j.chempr.2018.11.013

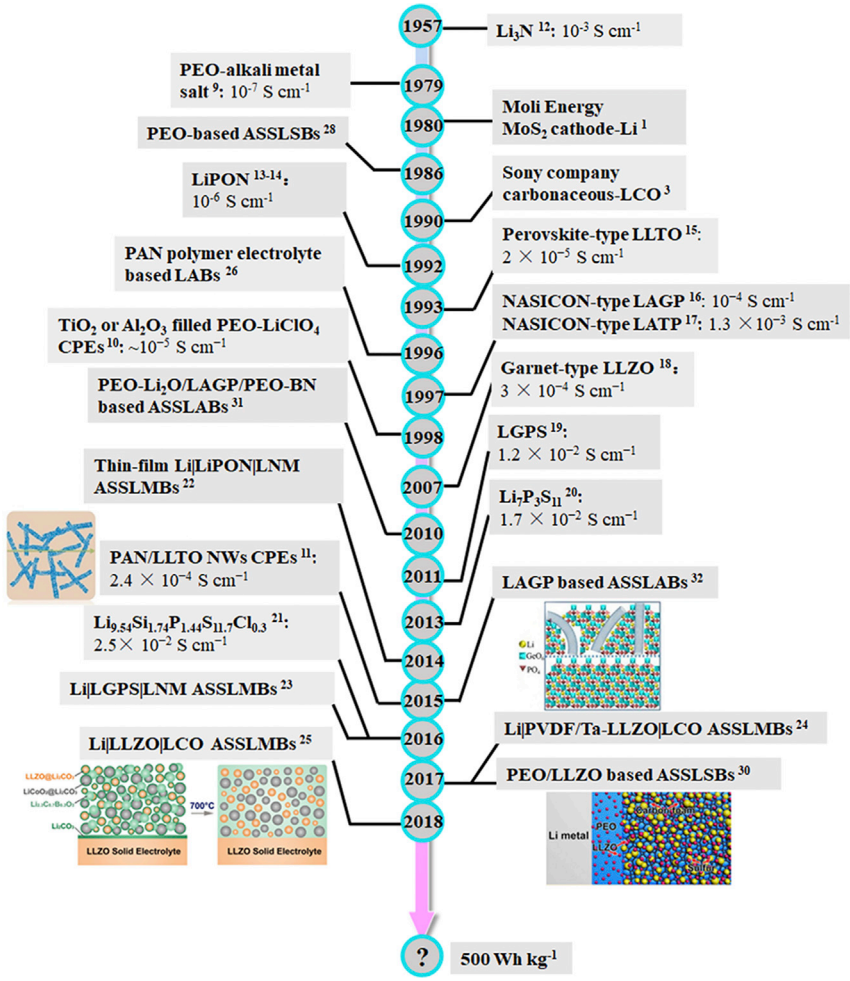

Figure 1. A Brief Chronology of the Development of Typical SSEs toward ASSLMBs

The application of SSEs by taking the place of liquid electrolyte in the Li batteries could fundamentally eliminate safety concerns. Besides, the electrochemical stability window of SSEs could reach as high as 5 V, and thus could be used with high-voltage cathode materials. Moreover, the possibility of utilizing the fascinating electrode materials with large specific capacities (i.e., Li metal, sulfur, and oxygen) is also appealing. SSEs in LIBs can generally be divided into three types: polymeric, inorganic, and composite materials. The concept of solid polymeric ionic conductor was begun in 1973 when Fenton et al. found that polyethylene oxide (PEO)-based complexes were alkali-metal-ion conductive.[8] Armand and co-workers then applied the complex of PEO and alkali metal salt as solid polymeric electrolytes (SPEs) in 1979, showing great application prospects,[9] which has spurred extensive research on SPEs for Li batteries in the subsequent 40 years (Figure 1). Early attempts to use SPEs were mainly based on the PEO system. In 1998, the pioneers Croce et al.[10] incorporated inorganic TiO_2 and Al_2O_3 fillers into the PEO-$LiClO_4$ matrix to construct composite polymer electrolytes (CPEs) of PEO-$LiClO_4$/TiO_2 and PEO-$LiClO_4$/Al_2O_3, showing remarkable ionic conductivities of $\sim 10^{-5}$ S cm^{-1} at 30°C, the highest reported data at that time. Their work paved the way for the practical application of CPEs for LIBs. It should be noted that the morphology of inorganic fillers in CPEs has a significant influence on the overall performance of

[1]School of Physical Science and Technology, ShanghaiTech University, Shanghai 201210, China

[2]Department of Materials Science and Engineering, Stanford University, Stanford, CA 94305, USA

[3]Stanford Institute for Materials and Energy Sciences, SLAC National Accelerator Laboratory, 2575 Sand Hill Road, Menlo Park, CA 94025, USA

[4]These authors contributed equally

*Correspondence: yicui@stanford.edu (Y.C.), liuwei1@shanghaitech.edu.cn (W.L.)

https://doi.org/10.1016/j.chempr.2018.11.013

Please cite this article in press as: Xia et al., Practical Challenges and Future Perspectives of All-Solid-State Lithium-Metal Batteries, Chem (2018), https://doi.org/10.1016/j.chempr.2018.11.013

the electrolyte. The most often used fillers are nanoparticles (NPs), which have challenges in forming effective ion transmission networks. In 2015, Liu et al.[11] first reported an effective strategy of constructing continuous ion-conduction channels in the CPEs via the incorporation of $Li_{0.33}La_{0.557}TiO_3$ (LLTO) nanowires (NWs) in the polyacrylonitrile (PAN) matrix, exhibiting an outstanding ionic conductivity of 2.4×10^{-4} S cm^{-1} at room temperature (RT).

Meanwhile, inorganic SSEs have also been extensively exploited for LIBs since the first Li-ion conductor Li_3N with a high ionic conductivity of 10^{-3} S cm^{-1} at RT but a low decomposition voltage of 0.445 V was discovered in the 1950s.[12] In 1992 a thin film-type Li phosphorus oxynitride (LiPON) was fabricated by Oak Ridge National Laboratory.[13,14] Inaguma et al. first demonstrated the Li-ion motion in perovskite-type $Li_{0.5}La_{0.5}TiO_3$ (LLTO) in 1993, showing a high conductivity of more than 2×10^{-5} S cm^{-1} at RT.[15] Later, in 1997 NASICON-type SSEs including $Li_{1+x}Al_xGe_{2-x}(PO_4)_3$ (LAGP) and $Li_{1+x}Al_xTi_{2-x}(PO_4)_3$ (LATP) were originally developed by Fu and co-workers, showing high ionic conductivities of 10^{-4} and 1.3×10^{-3} S cm^{-1}.[16,17] In 2007, a garnet-type fast ionic conductor of $Li_7La_3Zr_2O_{12}$ (LLZO) was originally reported by Murugan et al.,[18] with exciting properties such as an excellent ionic conductivity of 3×10^{-4} S cm^{-1} at RT and good thermal and chemical stability, showing great promise for all-solid-state Li batteries (ASSLBs). In 2011, Kanno's research group[19] first reported a Li superionic conductor of $Li_{10}GeP_2S_{12}$ (LGPS) showing a high ionic conductivity of 1.2×10^{-2} S cm^{-1} at RT, which rivaled that of liquid electrolyte. Their work was a landmark of the development history of SSEs and paved the way for fabricating high-power and -density energy-storage system for practical application in electric vehicles. Later, in 2013, another sulfide electrolyte of $Li_7P_3S_{11}$ was reported to show a higher ionic conductivity of 1.7×10^{-2} S cm^{-1}.[20] Then in 2016 an exceptional superionic conductor of $Li_{9.54}Si_{1.74}P_{1.44}S_{11.7}Cl_{0.3}$ was also reported by the Kanno group, showing the highest RT ionic conductivity of 2.5×10^{-2} S cm^{-1} to date.[21]

The development of SSEs with high ionic conductivities is expected to lead to the practical application of ASSLBs, especially all-solid-state LIBs (ASSLMBs) based on Li-metal anodes. In 2014, Dudney's group demonstrated the feasibility of high-voltage ASSLMBs using LiPON solid electrolyte, $LiNi_{0.5}Mn_{1.5}O_4$ (LNM) cathode and Li-metal anode, although bulk-type ASSLMBs with high loading of active materials and low cost will be required.[22] Later, Kanno's group[23] revealed the feasibility of operating bulk-type high-voltage Li|LGPS|LNM ASSLMBs at RT showing an initial discharge capacity of 80 mAh g^{-1} with an average voltage of 4.3 V at RT. Zhang et al.[24] reported high-performance poly(vinylidene fluoride) (PVDF)-$Li_{6.75}La_3Zr_{1.75}Ta_{0.25}O_{12}$ (Ta-LLZO) CPEs for Li|PVDF/Ta-LLZO|LCO ASSLMBs fabrication, showing excellent rate performance and good cycling stability. Very recently, Li|LLZO|LCO ASSLMBs have been reported by Wang's group[25] to exhibit both excellent cycling stability and high rate capability with cathode-electrolyte interface modification by incorporation of $Li_{2.3}C_{0.7}B_{0.3}O_3$ solder, which is the best performance to date. Their work is an important step toward promoting the practical use of SSEs.

Furthermore, "beyond Li" energy storages such as Li-S and Li-air batteries have attracted considerable interest due to their high theoretical capacities and energy densities. The research on Li-S batteries can be dated back to the 1940s; however, several challenges of insulating sulfide, Li_2S, Li_2S_2, and the shuttle effect of polysulfide restricted their development. Li-air batteries also have been investigated extensively since the first report in 1996 by Abraham and co-workers[26] based on organic polymer electrolyte and their later development by Bruce and co-workers.[27]

Please cite this article in press as: Xia et al., Practical Challenges and Future Perspectives of All-Solid-State Lithium-Metal Batteries, Chem (2018), https://doi.org/10.1016/j.chempr.2018.11.013

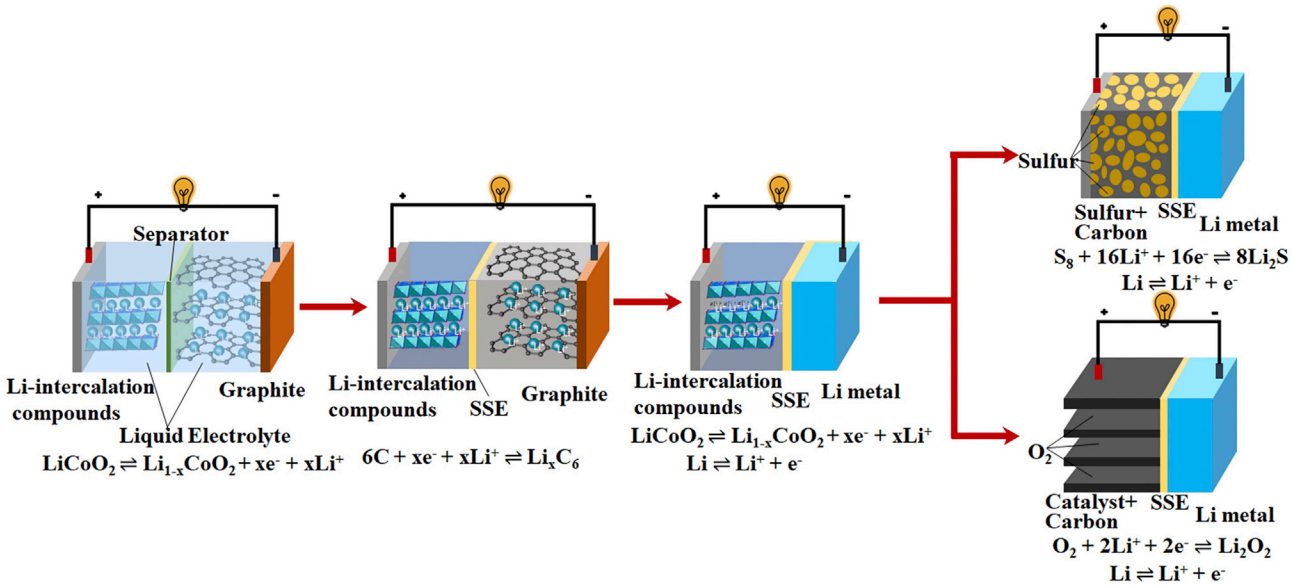

Figure 2. Schematic Diagram of the Development Trends of Li Batteries from Conventional LIBs to ASSLIBs Using Solid-State Electrolyte and then to Advanced Batteries Such as ASSLMBs, ASSLSBs, and ASSLABs Based on Li-Metal Anodes

However, these high-energy-density batteries suffer from serious problems, such as the shuttle effect of soluble polysulfide in Li-S batteries, leading to accumulation of insulating layers on the anode and poor cycling performance, and the degradation of the non-aqueous electrolyte and the corrosion of Li-metal anode in the open structure by ambient atmosphere in Li-air batteries. Accordingly, developing SSEs in Li-S and Li-air batteries by replacing conventional liquid electrolytes is quite attractive, as depicted in Figure 2 showing the schematic of the structural evolution of Li batteries. The early demonstrations of the all-solid-state Li-S batteries (ASSLSBs) were based on PEO polymeric electrolytes[28] and inorganic sulfide glass electrolytes.[29] Recently, Cui's group[30] reported ASSLSBs based on PEO/LLZO CPEs and sulfur composite cathode of S@LLZO@C, showing an appealing capacity of 900 mAh g^{-1}, high Coulombic efficiency (CE), and stable cycling performance at 37°C. In the context of developing all-solid-state Li-air batteries (ASSLABs), Kumar's group are the pioneers. They have fabricated ASSLABs based on glass-ceramic and polymer-ceramic materials exhibiting long cycle life (Figure 1),[31] greatly contributing to the fabrication of advanced energy-storage devices with ultra-high energy density. Years later, Zhou's group[32] used LAGP SSEs for constructing Li|LAGP|single-walled carbon nanotubes (SWCNTs)/LAGP ASSLABs, showing a high initial specific capacity of ~2,800 mAh g^{-1}. They found that the obtained ASSLABs with SWCNTs-LAGP composite cathode showed superior cycling performance compared with those with multi-walled carbon nanotubes (MWCNTs)-LAGP cathode with a reversible capacity of ~1,000 mAh g^{-1} at a current density of 200 mA g^{-1}.

However, to date ASSLMBs that can run stably at RT with high energy and power density have not been demonstrated, which is due to the low ionic conductivity as well as the large interfacial impedances of Li-electrode interfaces. The latter issue from the poor chemical, electrochemical, and physical compatibility of SSEs with electrodes is more critical in determining the electrochemical performances of ASSLMBs, especially the power density. All over the world many programs support the development of high-energy-density Li batteries. In the United States, Battery 500 Consortium's target is to make a battery pack with 500 Wh kg^{-1}, i.e., about twice

Please cite this article in press as: Xia et al., Practical Challenges and Future Perspectives of All-Solid-State Lithium-Metal Batteries, Chem (2018), https://doi.org/10.1016/j.chempr.2018.11.013

that of the currently commercial offerings. This goal will only be achieved by focusing on advanced batteries based on Li-metal anodes. exploring the use of LIBs in large energy-storage systems with high energy density, good rate capability, improved safety, and low cost for applications such as electric vehicles, and high cyclability, high efficiency, and low maintenance for grid storage.

In this review we discuss the main challenges and recent developments of the highly conductive SSEs including polymeric, inorganic, and composite materials for the next-generation high-energy-density Li batteries from fundamental understanding to technological innovation. The electrical performances of the composite solid electrolytes (CSEs) are comprehensively summarized. The strategies on the issues of SSE-electrode interface are later highlighted. In addition, the current progress and practical challenges of ASSLBs of Li-metal anodes coupled with Li-intercalation-compound, sulfur, and oxygen cathodes are presented. Lastly, future perspectives on ASSLMBs based on Li-metal anodes are also discussed.

SOLID-STATE ELECTROLYTES FOR LITHIUM BATTERIES

Functioning as not only an ionic conductor but also a separator, SSE holds great promise to promote the development of high-energy Li batteries with improved safety. Although SSEs are promising candidates to improve the overall performance of batteries, many critical issues need to be resolved for real-world applications:

(1) The low ionic conductivities of SSEs, especially at low temperatures
(2) The large interfacial resistance at the electrode-electrolyte solid-solid interfaces
(3) The poor electrochemical compatibility with electrodes, such as Li-metal anodes and high-voltage cathode materials
(4) The degraded physical stability with electrodes leading to large interfacial stress variation

Fundamental Understanding of Solid-State Electrolytes

Mechanism of Lithium-Ion Transport in Solid-State Electrolytes

Li-ion transport in SSEs can be mainly classified into two types: ion transport in polymeric and inorganic materials. The temperature dependence of ionic conductivity in SSEs is usually modeled by the Arrhenius (for crystalline materials) or Vogel-Tammann-Fulcher (VTF) equations (for amorphous materials).[33] The Arrhenius equation is

$$\sigma_i = \frac{A}{T}\exp\left[-\frac{E_a}{kT}\right], \qquad \text{(Equation 1)}$$

where A refers to the pre-exponential factor, k is the rate constant, and E_a is the activation energy for conductivity. The ionic conductivity in SPEs is usually modeled by the VTF equations with non-linear relationship due to the ion conduction involving ion hopping associated with the motion of polymeric chains,[34] and the equation is

$$\sigma_i = \sigma_0 T^{-\frac{1}{2}}\exp\left[-\frac{B}{T-T_0}\right], \qquad \text{(Equation 2)}$$

where B is the pseudo-activation energy, σ_0 is the pre-exponential factor, and T_0 is the reference temperature.

In SPEs it is commonly accepted that the ionic conduction is realized by the ions hopping from one coordinating site to another under an electrical field with the assistance of the segmental motion of polymer chains in amorphous phase above

Please cite this article in press as: Xia et al., Practical Challenges and Future Perspectives of All-Solid-State Lithium-Metal Batteries, Chem (2018), https://doi.org/10.1016/j.chempr.2018.11.013

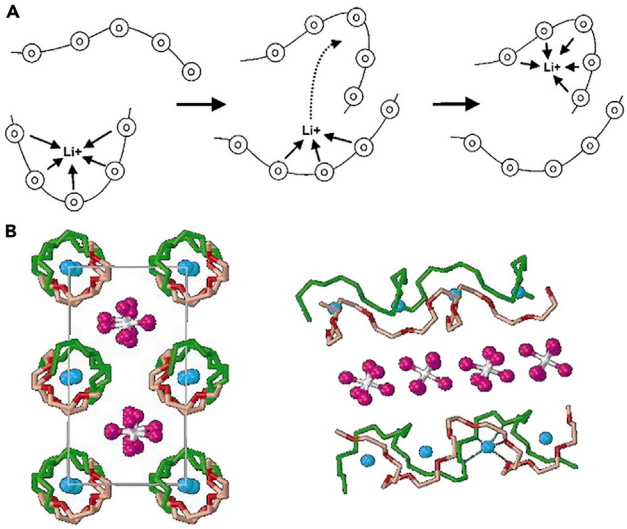

Figure 3. Schematic Illustration of Two Types of Li-Ion-Conduction Mechanisms for SPEs
(A) Li-ion conduction in amorphous phase of SPE. Reprinted with permission from Meyer.[35] Copyright 1998 Wiley-VCH Verlag GmbH & Co. KGaA.
(B) Li-ion conduction in crystalline phase of SPE.
Reprinted with permission from MacGlashan et al.[36] Copyright 1999 Springer Nature.

the glass transition temperature (T_g), as illustrated in Figure 3A.[35] Hence, the ionic conductivity of SPEs is strongly dependent on their crystallinity. Figure 3B shows the crystal structure of crystalline polymer electrolyte of PEO_6-$LiAsF_6$. Pairs of PEO chains are folded together forming cylindrical tunnels where Li ions are located inside via coordination with ether oxygens.[36] The Li-ion migration is achieved along the cylindrical tunnels with no need of the segmental motion of the polymer chains.

For crystalline inorganic materials, the Li-ion transport is achieved by their defect sites, and the concentration and distribution of defect sites can influence the ionic diffusion. The ionic diffusion mechanism based on Schottky and Frenkel point defects can be divided into two categories: vacancy-mediated mechanism (including vacancy and divacancy mechanism) and non-vacancy-mediated mechanism (including interstitial mechanism, interstitial-substitutional exchange mechanism, and collective mechanism).[37] It is reported that larger activation energy is required for vacancy-mediated mechanism compared with non-defect-mediated mechanism due to the extra requirement of vacancy formation energy. For ionic transport in glassy inorganic materials, it is quite similar to those with crystal structure. The macroscopic-scale ion transport is realized by excited ions moving from the local site to the other neighboring site.

Lithium-Ion Transport at the Electrolyte-Electrode Interface

Another issue that hinders the development of ASSLBs is the high interfacial resistance between electrolyte and electrode, which has a more significant influence on the overall performance of the battery.[38] The electrochemical reactions of ASSLBs are different from those Li batteries using liquid electrolyte with solid-liquid interface, which perform through the solid-solid electrolyte-electrode interface. Li ions diffuse from electrolyte to electrode through their interconnected region, and redox reaction with active materials and electrons occurs at the contacted electrolyte-electrode interface. Thus, it is critical to keep an effective solid-solid electrolyte-electrode interface all the time in batteries to guarantee that the charge-transfer reaction stably proceeds.

Please cite this article in press as: Xia et al., Practical Challenges and Future Perspectives of All-Solid-State Lithium-Metal Batteries, Chem (2018), https://doi.org/10.1016/j.chempr.2018.11.013

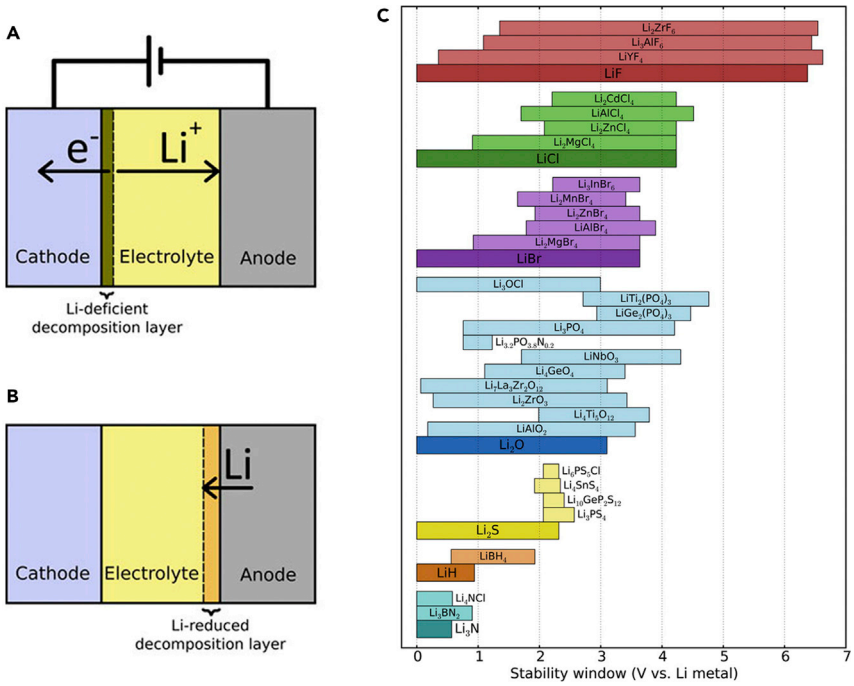

Figure 4. Schematics of the Electrode-Electrolyte Interface and the Electrochemical Stability Windows of SSEs

(A) Li-deficient layer formed at the cathode-electrolyte interface.

(B) Li-reduced decomposition layer faced with Li-metal anode.

(C) Electrochemical stability windows of various SSE materials.

Reprinted with permission from Richards et al.[39] Copyright 2016 American Chemical Society.

The main contribution to the large interfacial resistance is from the chemical and electrochemical instability of SSEs with electrodes, for example, the space-charge layer of a local Li-ion-deficient layer in the electrolyte near the cathode (Figure 4A), due to the potential difference between cathode and electrolyte resulting in Li ions extracted from the electrolyte to the cathode side while strongly limiting the battery rate capability.[39] The space-charge layer, a natural bridge between the bulk properties and the neighboring phase, was usually used for explaining the conductivity in a heterogeneous system.[40] Oxide cathode materials were usually mixed conductors with high ionic conductivity, whereas sulfide electrolytes were single Li-ion conductors. When oxide cathode materials contact with sulfide solid electrolytes, Li ions are prone to transfer from the sulfide electrolyte to oxide electrode side due to their large electrochemical potential difference. The space-charge layer at the cathode side can be alleviated by the electronic conduction while the Li ions continue moving toward the cathode side, resulting in further enlargement of the space layer. Consequently, a large interfacial resistance is formed at the electrolyte-cathode interface.[40] For the interface between Li-metal anode and electrolyte, the side reaction that produces the solid electrolyte interface (SEI) layer could also increase the interfacial resistance (Figure 4B), whereas only a few SSEs show good stability against the highly active Li-metal anode. Schwöbel and co-workers[41] first found that LiPON could react with Li metal to form the decompositions including Li_3PO_4, Li_3P, Li_3N, and Li_2O. A stable passivation layer with the ability of conducting Li ions and blocking further reaction obtained at the interface could be a benefit. In addition, with a wide electrochemical window, SSEs that are thermodynamically stable at the Li chemical potential range between the anode and the cathode are required in LIBs. The electrochemical stability ranges of current widely studied SSEs are presented in Figure 4C.

Please cite this article in press as: Xia et al., Practical Challenges and Future Perspectives of All-Solid-State Lithium-Metal Batteries, Chem (2018), https://doi.org/10.1016/j.chempr.2018.11.013

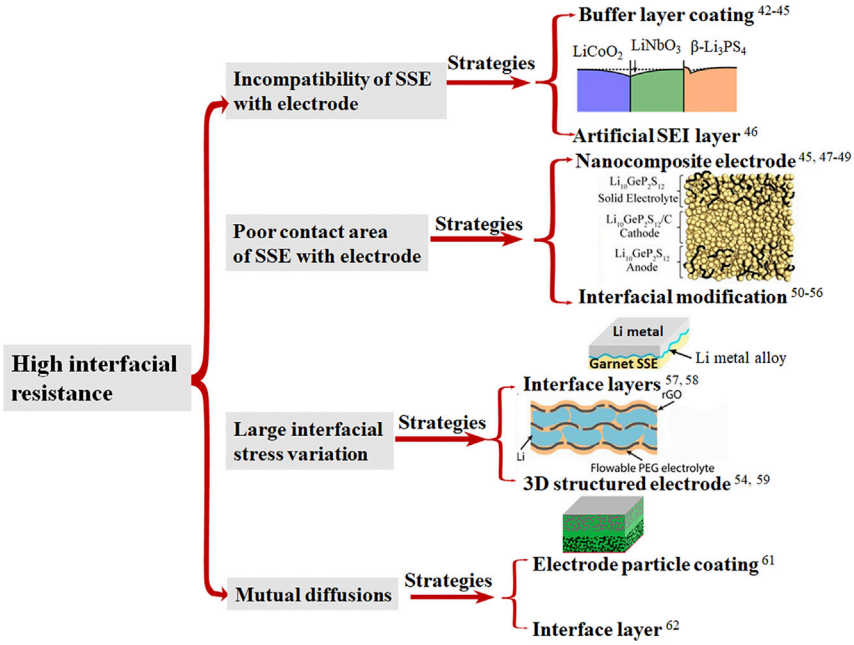

Figure 5. Strategies for Reducing High Solid-Solid Interfacial Impedances

Besides and obviously, unlike the liquid electrolyte that has good wettability with electrodes, the contact between SSE (especially the inorganic solid electrolytes) and electrode is poor. Moreover, the volume changes of cathode and anode materials during repeated charging and discharging could lead to the loss of effective contact between the electrode and SSE, which limits the conduction of Li ions across the interface region and the subsequent cycling performance of the battery. Additionally, it should be noted that the element mutual diffusion layer formed at the electrolyte-electrode interface is also a significant resistor to deteriorating interface stability upon cycling. Because oxide-based solid electrolytes are physically inflexible, the battery fabrication process usually requires an additional heating step to improve adhesion between electrode and electrolyte. As a result, the element mutual diffusion region occurs at the solid-solid interface, accompanied by formation of a significant inevitable interfacial resistance. Various approaches have been proposed to address these issues, as illustrated in Figure 5.

The interfacial resistances are mainly attributed to the incompatibilities of SSE with electrodes due to the space-charge effect, chemical and electrochemical instability, interdiffusion, and so forth. Incorporation of an ion-conducting and electron-insulting buffer layer coating on electrode particles is an effective approach to reduce the incompatibilities. Various buffer thin films such as $Li_4Ti_5O_{12}$ (LTO),[42] $LiNbO_3$,[43] and Al_2O_3[44] have been proposed as a coating on LCO to reduce the interfacial impedance with sulfide electrolyte by weakening the space-charge effect. Ohta et al.[42] found that the rate capability of ASSLMBs based on sulfide electrolyte could be significantly improved by coating LCO particles with LTO, due to reduced space-charge layer effect. In addition, electrochemical stability of SSEs against electrode materials under applied potential is a crucial factor affecting the performance of ASSLBs. Kitaura et al.[45] found that a reaction of LCO with the $80Li_2S{\cdot}20P_2S_5$ glass solid electrolyte occurred during the hot press, which could degrade the obtained battery performance, and the electrochemical stability of electrolyte with electrode could be improved with a $LiNbO_3$

Please cite this article in press as: Xia et al., Practical Challenges and Future Perspectives of All-Solid-State Lithium-Metal Batteries, Chem (2018), https://doi.org/10.1016/j.chempr.2018.11.013

buffer layer coating on LCO particles. The hot press-derived ASSLBs of LTO|80Li_2S•20P_2S_5|$LiNbO_3$-coated LCO demonstrated a high specific capacity of 120 mAh g^{-1} at 0.064 mA cm^{-2} at RT. To reduce the interface instability, introducing an artificial SEI layer of electronic insolation and ionic conduction is also an effective approach. Goodenough's group[46] demonstrated that an ion-conducting passivation layer consisting of Li_3P and Li_8ZrO_6 could be formed *in situ* for the solid electrolyte of $LiZr_2(PO_4)_3$ contacting Li metal.

Increasing the contact area of electrode with electrolyte via the nanocomposites of electrode and electrolyte is one often used effective approach, using techniques such as ball-milling,[47] pulsed laser deposition (PLD),[48] and softening the glass electrolyte.[45] Hayashi et al.[47] reported that the contact area of solid-solid interface between the electrode and electrolyte was remarkably improved by using mechanochemical balling to obtain electrode-electrolyte nanocomposites. The obtained ASSLBs based on this nanocomposite of NiS-80Li_2S•20P_2S_5 demonstrated a larger initial discharge capacity of 770 mAh g^{-1} at 1.3 mA cm^{-2} and better cycling performance with a capacity of 360 mAh g^{-1} for 50 cycles than those with electrodes by the conventional hand-mixing method. Wang's group[49] also reported an ASSLB with a single material of LGPS acting as cathode, anode, and electrolyte to completely address the interfacial resistance issues. The proposed new concept of the single-material battery is a promising direction to circumvent the toughest interfacial problem. As for the anode-electrolyte interface, coating the softening 80Li_2S•20P_2S_5 glass electrolyte onto the LTO active-material particles is reported by Tatsumisago's group to increase the contact area of the active material and solid electrolyte.[45] By heating at around the glass transition temperature of electrolyte and then cooled down to RT, a favorable electrolyte-electrode contact was achieved by sticking the electrolyte onto the active electrode materials.

Interfacial modification is also a common approach to increase the effective contact area of electrolyte and electrode. Tatsumisago's research group[50] reported that insertion of Au thin film between Li metal and Li_2S-P_2S_5 SEI prepared by vacuum evaporation could improve the electrolyte-electrode interface and promote stable Li dissolution and deposition reactions with an achieved high utilization of Li-metal electrode as high as 40%. Notably, garnet-type LLZO SSEs are promising electrolyte candidates for their relatively high ionic conductivity (10^{-4}–10^{-3} S cm^{-1} at RT) and good stability against Li-metal anode. However, the poor contact at the electrolyte-electrode interface resulted in a high interfacial resistance and uneven current distribution. Hu's group from the University of Maryland has undertaken much research to reduce the interfacial resistance between garnet electrolyte and Li-metal anode.[51–56] In 2016, they[53] reported that introduction of an ultrathin Al_2O_3 coating on garnet-like $Li_7La_{2.75}Ca_{0.25}Zr_{1.75}Nb_{0.25}O_{12}$ via atomic layer deposition could dramatically improve both the wetting and stability of garnet-typed SSE against Li-metal anode, showing an exciting result of interfacial impedance significantly decreasing from 1,710 to 1 Ω cm^2. Their work has addressed the primary challenge of high interfacial resistance in garnet SSEs with Li-metal anode and is thus a significant breakthrough in the development of high-energy-density and safe ASSLBs. Later, various interface layers of ZnO,[54] amorphous Si,[55] polymer layer,[56] Ge,[51] and Al[52] were also proved by their group to showing the abilities of increasing the wettability of SSEs and reducing the interfacial resistance between garnet electrolytes with Li-metal anode.

The large interfacial stress variation resulted from the large volume changes of the electrodes during lithiation-delithiation cycles is also a serious problem. Introducing an

Please cite this article in press as: Xia et al., Practical Challenges and Future Perspectives of All-Solid-State Lithium-Metal Batteries, Chem (2018), https://doi.org/10.1016/j.chempr.2018.11.013

interface layer that could conformally contact with electrodes is an interesting method. Yamamoto et al.[57] reported that stress at the interface during delithiation could be effectively weakened by introduction of an NbO_2 layer at the LCO electrode-solid electrolyte interface. Recently, Cui's group[58] also reported constructing a flowable interfacial layer that could accommodate the interface fluctuation and ensure the effective and intimate contact of electrolyte and electrode, achieving conformal and continuous ionic contact between the electrode and electrolyte. To deal with the difficult large volume change of Li-metal anode during cycling, resulting in poor contact between Li metal and SSEs, Hu et al.[54,59] proposed a self-standing Li-metal anode by using 3D porous LLZO SSEs to act as a host matrix of Li-metal anode, which could maintain good battery cycling stability during the Li-ion plating-stripping process.

The migration of chemical elements at the interface of SSE and electrode is also a critical factor in determining the electrochemical performances of the resultant ASSLMBs. Brazier et al.[60] first adopted *ex situ* transmission electron microscopy (TEM) to observe the diffusion of heavy elements across the SSE-LCO interface. To address the element mutual diffusion occurring at the electrolyte-electrode interface, researchers have suggested interfacial modification. Sakuda et al.[61] demonstrated that the element mutual diffusion between LCO and sulfide electrolyte was suppressed using Li_2SiO_3 coatings on LCO particles. The ASSLBs using Li_2SiO_3-coated LCO could be charged and discharged reversibly under a significantly high current density of 40 mA cm^{-2}. Kato et al.[62] introduced a thin Nb layer (~10 nm) between LLZO and LCO, showing an obviously suppressed mutual diffusion layer. The Nb interlayer dramatically improved both the discharge capacity and rate capability of the batteries.

Observation of the Electrolyte-Electrode Interface

Understanding and improving the behavior of the electrolyte-electrode interface with nanoengineering and materials design technology is absolutely necessary for constructing a safe Li battery with improved electrochemical performance. Observing the interface evolution occurring in a battery in real time at the atomic scale is a long-standing dream for scientists. Brazier et al.[60] first applied *ex situ* TEM for the observation of solid-solid interface with a focused ion beam, and their achievements paved the technical way for *in situ* observation. Recently, Wang et al.[63] explored the solid-solid electrolyte-electrode interfacial phenomenon with *in situ* scanning transmission electron microscopy (STEM) coupled with electron energy loss spectroscopy (EELS) (Figure 6A). They demonstrated that the mechanism of interfacial impedance at the LCO-LiPON interface was caused by chemical changes rather than space-charge effects, whereas the large interfacial resistance from the space-charge layer was confirmed by quantitative electron holography (EH) operated by TEM. It was found that an obvious drop and a gradual reduction of potential was formed at the interface of LCO cathode and inorganic electrolyte in an ASSLB during charge-discharge cycles, which leads to high resistance to Li-ion transport (Figure 6B).[64] Moreover, Chueh's group[65] applied an X-ray microscopy platform to investigate the Li composition dynamics and insertion rate in LFP (Figure 6C), finding that the lithiation pathway was controlled by the nanoscale spatial variations in rate and composition. Li composition coupled with surface reaction rates could also control the kinetics and uniformity of Li-ion insertion reactions at the interface. It should be highlighted that very recently, Cui's group[66] demonstrated the atomic image of Li metal by using cryo-TEM (Figure 6D), which is a breakthrough with respect to the observation and microstructure of Li metal and the SEI layer. In the near future, this technology may be used to investigate the solid-solid electrolyte-electrode interface.

Please cite this article in press as: Xia et al., Practical Challenges and Future Perspectives of All-Solid-State Lithium-Metal Batteries, Chem (2018), https://doi.org/10.1016/j.chempr.2018.11.013

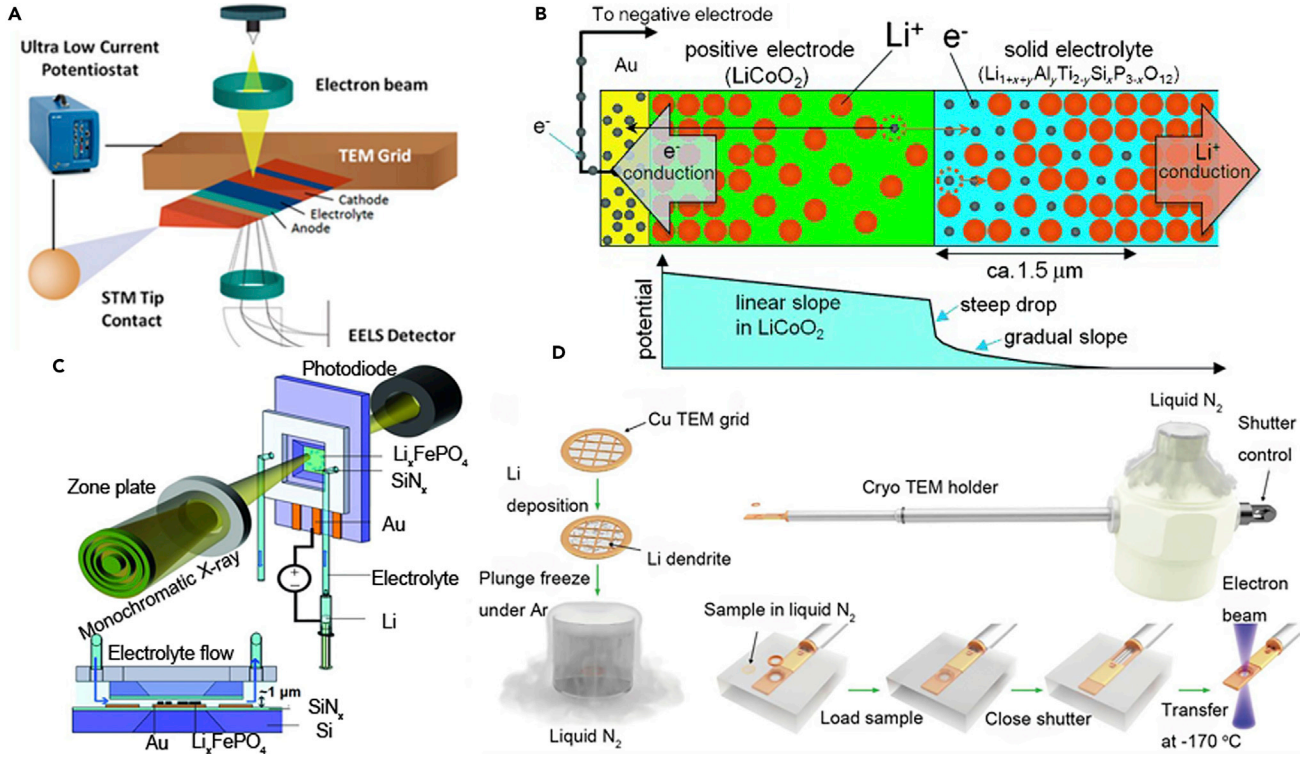

Figure 6. Microstructure and Morphology of the Electrolyte-Electrode Interfaces by Various Advanced Technologies

(A) Setup for *in situ* STEM. Reprinted with permission from Wang et al.[63] Copyright 2016 American Chemical Society.

(B) The distribution of Li-ions and electrons at the electrode-electrolyte interface under the charged state (top), and measured potential distribution (bottom), based on EH operated by TEM. Reprinted with permission from Yamamoto et al.[64] Copyright 2010 Wiley-VCH Verlag GmbH & Co. KGaA.

(C) The *operando* liquid imaging platform for X-ray microscopy. Reprinted with permission from Lim et al.[65] Copyright 2016 AAAS.

(D) Procedures for the characterization by cryo-TEM. Reprinted with permission from Li et al.[66] Copyright 2017 AAAS.

Solid-State Electrolytes

Solid Polymer Electrolytes

SPEs based on dry polymers with dissolved Li salt show superior advantages over inorganic solid electrolyte in terms of flexibility, light weight, good processability, and low cost. Li salts ($LiClO_4$, $LiPF_6$, $Li[N(SO_2CF_3)_2]$, etc.) are solvated in polymer matrix such as PEO,[67] PAN,[68] poly(methyl methacrylate) (PMMA),[69] PVDF,[68] poly (ethylene carbonate) (PEC),[70] and poly(propylene carbonate) (PPC)[71] to realize Li-ion conduction. The research on SPEs dates back to 1973 when Wright et al.[8] first discovered that PEO coordinated with alkali metal salt and the resulting complex is ion conductive. The early investigation of SPE was mainly focused on PEO and its derivatives, which are the most widely studied polymers due to their superior ability to dissolve Li salts.[10] Unfortunately, the ionic conductivity of PEO-based SPEs is only 10^{-7}–10^{-5} S cm^{-1} at RT and their low conductivity is mainly due to the low degree of chain mobility for their partial crystallization below 60°C. Different approaches have been proposed to enhance the ionic conductivity of SPEs due to either the reduction of the crystallinity of the polymers or the fast interfacial conduction, including incorporation of ceramic fillers,[72] plasticizer,[73] polymer blend,[74] copolymerization,[67,75] adding of the metal-organic framework (MOF) NPs,[76] and organic robust cage.[77]

Generally, SPEs are dual-ion conductors in which Li-ion and its counter anions are both mobile. For this reason Li-ion is coupled with Lewis basic sites of the polymer

Please cite this article in press as: Xia et al., Practical Challenges and Future Perspectives of All-Solid-State Lithium-Metal Batteries, Chem (2018), https://doi.org/10.1016/j.chempr.2018.11.013

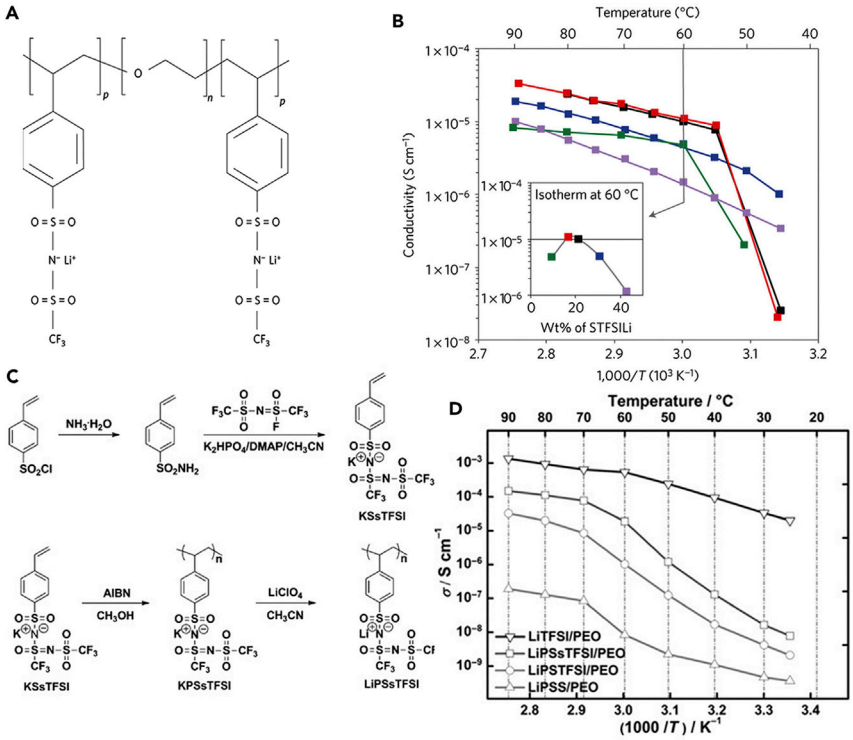

Figure 7. Single-Ion Polymer Electrolytes and Their Corresponding Conductivity Performances

(A and B) Chemical structure of the single-ion-conducting polymer electrolyte (A) and conductivity performance of polymer electrolytes with different proportions of P(STFSILi) (B). Green, 9.5 wt %; red, 17 wt %; black, 21.4 wt %; blue, 31 wt %; purple, 43 wt %. Inset: isothermal conductivity at 60°C. Reprinted with permission from Bouchet et al.[80] Copyright 2013 Springer Nature.

(C and D) The synthesis route of single Li-ion-conducting LiPSsTFSI polymer (C) and conductivity performance of different electrolytes (D). Reprinted from Ma et al.[81] Copyright 2016 Wiley-VCH Verlag GmbH & Co. KGaA.

matrix, and thus Li-ion is usually less mobile than anion. As a result, the Li-ion transference number (LTN) of ionic conductors with dual ions is generally lower than 0.5.[78] In conventional SPE, Li-ion and its counter anions move oppositely during the discharge cycles, leading to the anions tending to accumulate at the anode side causing concentration gradients and cell polarization, and subsequently deteriorating the battery performance.[79] However, single Li-ion conductive SPEs could display almost unity LTN thanks to their anions being immobilized by anion acceptors or polymer backbones, which have attracted great attention because of their lack of anion polarization deleterious effect. Nevertheless, it is quite difficult for this kind of material to have properties of both high ionic conductivity and good mechanical strength. In 2013, self-assembled polyanionic triblock co-polymers based new single-ion polymer electrolytes were reported for fabricating ASSLBs by Bouchet et al.[80] (Figure 7A), showing a high ionic conductivity of 1.3×10^{-5} S cm^{-1} at 60°C (Figure 7B), a markedly improved mechanical strength, and an enlarged electrochemical window as high as 5 V versus Li^+/Li. Their work paved the way for elaborating high-performance macromolecular electrolytes for ASSLBs. To further improve the ionic conductivity, Ma et al.[81] recently reported a novel single Li-ion-conducting PEO-based polymer electrolyte by simply dissolving Li salt of poly[(4-styrenesulfonyl)(trifluoromethyl(*S*-trifluooromethylsulfony-limino)sulfonyl)imide] ($PSsTFSI^{-1}$) in PEO matrix (Figure 7C). This material exhibited a high LTN of 0.91 and a high ionic conductivity of 1.35×10^{-4} S cm^{-1} at 90°C, comparable with that of the classic

Please cite this article in press as: Xia et al., Practical Challenges and Future Perspectives of All-Solid-State Lithium-Metal Batteries, Chem (2018), https://doi.org/10.1016/j.chempr.2018.11.013

PEO-Li[$N(SO_2CF_3)_2$] (LiTFSI) electrolyte (Figure 7D). Recently, Zhang et al.[82] fabricated an sp^3 boron-based solid single-ion-conducting polymer electrolyte for ASSLB fabrication and the fabricated full batteries displayed excellent electrochemical performance even operating at a temperature as low as 50°C below the melting point of PEO, which has never been reported so far for ASSLBs based on single-ion-conducting polymer electrolytes. Their work made a significant step toward fabricating SPE-based ASSLBs operating at RT in the near future.

Inorganic Solid Electrolytes

The main inorganic solid Li-ion conductors include garnet-type, perovskite-type, sodium superionic conductor (NASICON)-type, and Li superionic conductor (LISICON)-type materials, and sulfide glasses, among others. In general, they can be divided into two categories, oxides and sulfides, which are discussed in detail in this section.

Oxides. The general formula of garnet-type materials is $A_3B_2(XO_4)_3$ (A = Ca, Mg, Y, La or rare earth; B = Al, Fe, Ga, Ge, Mn, Ni, V; X = Si, Ge, Al), where the A and B cations have 8-fold and 6-fold coordination, respectively. In 2003, Thangadurai et al.[83] firstly reported a novel class of fast Li-ion-conducting oxides $Li_5La_3M_2O_{12}$ (M = Nb, Ta) possessing garnet-like structures. In the following years, the conductivity optimization was continuously done by chemical substitutions or structural modifications. In 2007, Murugan et al.[18] synthesized a new garnet-type material with molecular composition of LLZO showing an extraordinarily high ionic conduction of 3×10^{-4} S cm^{-1} at RT. Since then, LLZO and its derivates have been widely investigated for ASSLMB construction because of their relatively high ionic conductivity and good chemical stability against Li-metal anode. Years later, Awaka et al.[84] determined the detailed crystal structure of cubic LLZO (Figures 8A and 8B) by single-crystal X-ray structure analysis. It was detected that a 3D network of the Li-ion migration pathway with short Li-Li distance and occupational disordering is formed in the garnet-type framework structure. The basic unit of the pathway is a loop constructed by the Li1 and Li2 sites. Generally, LLZO of tetragonal phase exhibits two orders lower conductivity compared with its corresponding cubic phase,[85] and in order to obtain a higher conducting cubic phase structured LLZO, a small amount of Ta,[87] Al,[88] Ga,[88] Nb,[89] or Te[90] was usually doped. Particularly, $Li_{6.4}La_3Zr_{1.4}Ta_{0.6}O_{12}$ showed an extremely high Li-ion conductivity of $\sim 10^{-3}$ S cm^{-1} among the known Li-stuffed garnets at RT with an activation energy of 0.35 eV.[18,87] Deviannapoorani et al.[90] then reported that a high total (bulk and grain boundary) ionic conductivity of 1.02×10^{-3} S cm^{-1} could be achieved at 30°C for $Li_{6.5}La_3Zr_{1.75}Te_{0.25}O_{12}$ compounds sintered at 1,100°C by substitution of Zr^{4+} by Te^{6+} in the garnet lattice of LLZO. Recently, Guo's group[91] demonstrated that the highest ionic conductivity of 1.46×10^{-3} S cm^{-1} at RT to date with a low activation energy of 0.25 eV was found for the composition of $Li_{7-3x}Ga_xLa_3Zr_2O_{12}$ at $x = 0.25$ by solid-state reaction. Garnet-type solid electrolytes show high ionic conductivity and wide electrochemical window; however, faced with moisture they are not stable, undergoing the Li^+/H^+ exchange at RT resulting in an insulating Li_2CO_3 coating layer.[92]

The ideal general formula of perovskite structure is ABO_3 (A = Li, La; B = Ti), where A sites are in 12-fold coordination and B sites are in 6-fold coordination. Figure 8C shows the crystal structure of tetragonal $Li_{3x}La_{(2/3)-x}\square_{(1/3)-2x}TiO_3$ (LLTO, $0 < x < 0.16$, $\square$ represents a vacancy), which could show a high bulk conductivity of 10^{-3} S cm^{-1};[86] however, the total ionic conductivity of the battery could only reach 10^{-5} S cm^{-1} due to the high grain boundary resistance.[15] It could be detected that LLTO is composed of cubic phase α-LLTO with *Pm3m* symmetry and tetragonal

Please cite this article in press as: Xia et al., Practical Challenges and Future Perspectives of All-Solid-State Lithium-Metal Batteries, Chem (2018), https://doi.org/10.1016/j.chempr.2018.11.013

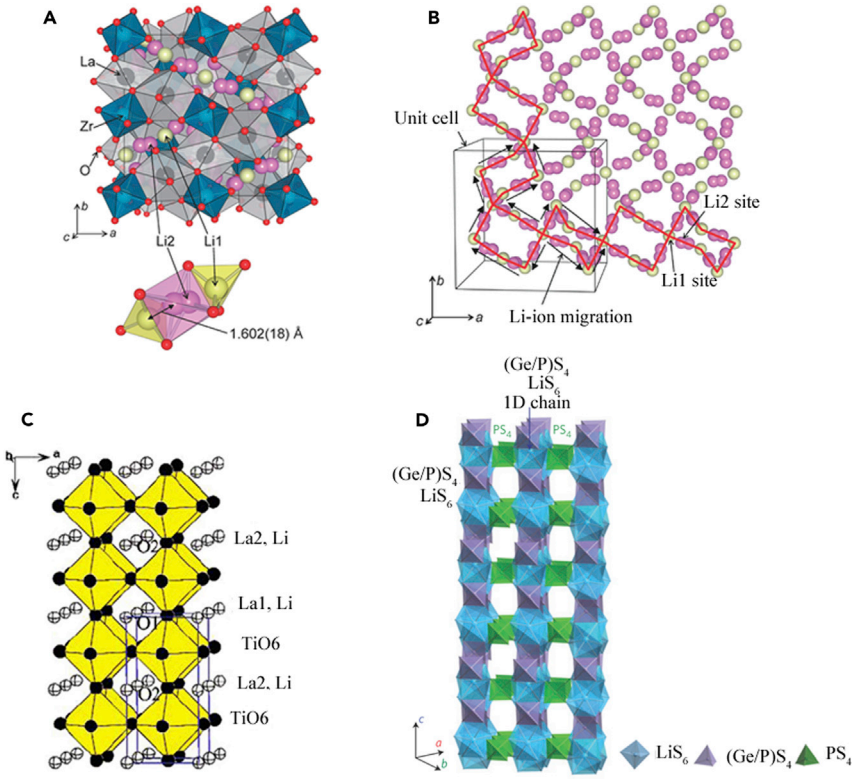

Figure 8. Crystal Structures of Represented Inorganic Materials

(A and B) Crystal structure of cubic $Li_7La_3Zr_2O_{12}$ (A) and three-dimensional conducting network of Li atomic arrangement in cubic $Li_7La_3Zr_2O_{12}$ (B). Reprinted from with permission from Awaka et al.[84] Copyright 2011 Chemical Society Japan.

(C) Crystal structure of $Li_{3x}La_{(2/3)-x}\square_{(1/3)-2x}TiO_3$. Reprinted with permission from Stramare et al.[86] Copyright 2003 American Chemical Society.

(D) Crystal structure of $Li_{10}GeP_2S_{12}$. Reprinted with permission from Kamaya et al.[19] Copyright 2011 Springer Nature.

phase β-LLTO with a *P4/mmm* space group. The conductivity of LLTO depended on the bottleneck size and site percolation. Increasing the bottleneck size by introducing large rare-earth or alkaline-earth metal ions in the A site significantly improved the ionic conductivity. It was reported that the increases in the bulk ionic conductivities could be observed at 400 K with inclusion of rare-earth metal ions (La^{3+} > PR^{3+} > Nd^{3+} > Sm^{3+}).[93] Because of the reduction of Ti^{4+} in LLTO faced with Li-metal anode, LLTO was thus not a suitable electrolyte candidate for batteries with Li-metal anode. In addition, anti-perovskites ABX_3 (A = Cl^-, Br^-, I^-; B = O^{2-}; X = Li^+) are also Li-rich superionic conductors.[94] Zhao et al.[94] demonstrated a novel class of Li-rich anti-perovskite-based solid electrolyte composed of 3D conducting pathways, showing a conductivity as high as 10^{-3} S cm^{-1} at RT with an activation energy of 0.2–0.3 eV.

Crystalline phosphate with NASICON-type structures such as $Li_{1+x}Al_xTi_{2-x}(PO_4)_3$ (LATP) and $Li_{1+x}Al_xGe_{2-x}(PO_4)_3$ (LAGP) are known as excellent Li-ion conductors with high ionic conductivities of ~7×10^{-4} S cm^{-1} at RT, wide electrochemical window of 6 V, and good stability with moist atmosphere. The conductivity of commercialized LATP could reach as high as 1.3×10^{-3} S cm^{-1}.[95] However, similarly to LLTO, these NASICON-type electrolytes are also unstable with Li-metal anodes. The crystalline structures of LISICON-type compounds are similar to that of

Please cite this article in press as: Xia et al., Practical Challenges and Future Perspectives of All-Solid-State Lithium-Metal Batteries, Chem (2018), https://doi.org/10.1016/j.chempr.2018.11.013

γ-Li_3PO_4, showing an orthorhombic unit cell and *Pnma* space group with all cations tetrahedrally coordinated.[96] However, the ionic conductivities of this kind of material were quite low, only $\sim10^{-7}$ S cm^{-1} at RT. Fast ion conductor $Li_{3+x}(P_{1-x}Si_x)O_4$ could be prepared by aliovalent substitution of P^{5+} in γ-Li_3PO_4 by Si^{4+}, showing a conductivity of 3×10^{-6} S cm^{-1}.

Sulfides. The earliest studied sulfide-type solid electrolyte was the Li_2S-SiS_2 system. The commonly used sulfide glass electrolytes include Li_2S-P_2S_5, Li_2S-GeS_2, Li_2S-B_2S_3, and Li_2S-SiS_2 with conductivities of $\sim10^{-4}$ S cm^{-1}. Thio-LISICON-type $Li_{3+x}(P_{1-x}Si_x)S_4$ obtained by substituting O element with S element showed improved ionic conductivity by 2–3 orders of magnitude at RT with a high ionic conductivity of 6×10^{-4} S cm^{-1}.[97] The crystalline structure of thio-LISICON was similar to that of γ-Li_3PO_4 with orthorhombic unit cell, where all cations are tetrahedrally coordinated.[96] Generally thio-LISICON electrolytes show higher conductivity and lower activation energy compared with LISICON materials. This is because sulfides have higher ionic radius than oxides, thus showing enlarged ionic transport channels. Moreover, the more polarizable character of sulfide ions could improve the mobility of the Li ions. Recently, Kamaya et al.[19] reported that LGPS with a new 3D framework structure exhibited an extremely high ionic conductivity of 1.2×10^{-2} S cm^{-1} at RT, even higher than that of liquid organic electrolytes. This material was reported to have many advantages with regard to safety, electrochemical properties, and battery fabrication. Figure 8D shows the framework structure of LGPS composed of $(Ge_{0.5}P_{0.5})S_4$ tetrahedra and LiS_6 octahedra connected to each other by a common edge, forming one-dimensional (1D) chains. These chains connect with PS_4 tetrahedra by a common corner.[19] Although LGPS showed a wide potential window of 4.0 V versus Li^+/Li, computational studies showed that this material was unstable faced with Li-metal reduction at low voltage, and the decomposition of LGPS accompanied by extraction of Li could happen at high voltage.[98] Later, Seino and co-workers[20] demonstrated that heat-treated Li_2S-P_2S_5 glass-ceramic electrolyte showed an extremely high ionic conductivity of 1.7×10^{-2} S cm^{-1} at RT. To date, for Li-ion solid conductors the highest ionic conductivity of 2.5×10^{-2} S cm^{-1} was observed in the chlorine-doped silicon-based sulfide electrolyte ($Li_{9.54}Si_{1.74}P_{1.44}S_{11.7}Cl_{0.3}$), and highly stable $Li_{9.6}P_3S_{12}$ was also reported to have high electrochemical stability of $\sim$0 V versus Li metal.[21] Ceder's group[99] applied a structural matching algorithm to fundamentally reveal a body-centered cubic-like anion framework allowing direct Li-ion hopping with a low activation barrier and high ionic conductivity, which is found in sulfide SSEs such as $Li_{10}GeP_2S_{12}$ and $Li_7P_3S_{11}$. However, sulfide-based SSEs are highly sensitive to moisture, resulting in the formation of hydrogen sulfide, which critically limits their commercialized applications.

Organic-Inorganic Composite Electrolytes

CSEs can be divided into two types according the dominant components: polymer matrix (CPEs) and inorganic material matrix. CPEs derived from SPEs with inorganic fillers usually show a higher ionic conductivity, improved mechanical property, and better compatibility with the electrodes, and thus have attracted intense scientific interest over the last decade. Constructing CPEs that could combine the advantages of both organic and inorganic electrolytes has been considered a promising approach to fabricate flexible batteries with high performance.[10] The enhanced mechanical properties help to prevent Li dendrite growth and improve safety. In this regard many polymers such as PAN,[100] and PMMA[69] coupled with various inorganic fillers have also been exploited. In particular, nanosized ceramic powders with large specific surface area have been utilized widely, including inert nanofillers such

Please cite this article in press as: Xia et al., Practical Challenges and Future Perspectives of All-Solid-State Lithium-Metal Batteries, Chem (2018), https://doi.org/10.1016/j.chempr.2018.11.013

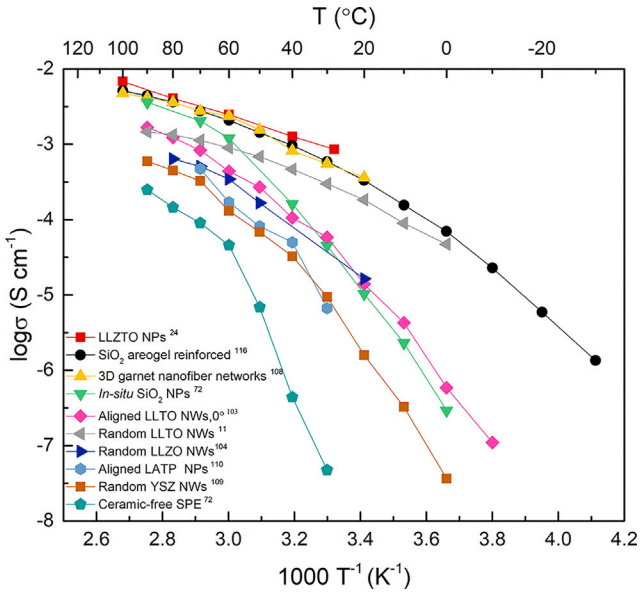

Figure 9. Comparison of Ionic Conductivities of CSEs in Recent Publications

as SiO_2,[73] TiO_2,[101] Al_2O_3,[100] $BaTiO_3$,[102] and active nanofillers such as LLTO[103] and LLZO.[104,105] Figure 9 shows a comparison of the conductivities of CPEs reported in some recent works, which will be introduced in the following subsections.

Two main theories are proposed to explain the mechanism of the enhanced ionic conductivities of CPEs compared with filler-free SPEs. It is believed by some that the inert nanofillers distributed in the polymer matrix could act as crosslinking centers hindering the reorganization of the polymer chain and thus lowering the polymer crystallinity and speeding up of segmental dynamics,[106] whereas others hold that the strong Lewis acid-base interaction of Li ions with the surficial chemical group of ceramic fillers could contribute to the dissociation of Li salts to achieve more free Li ions and a fast ion-conduction pathway on the filler's surface, consequently leading to the enhancement of conductivity of CPE.[107] Although these two explanations interpreted the mechanism from different aspects, some researchers believe they work together to obtain the final improvement.[72] For the active fillers, they can also directly participate in Li-ion conduction.

Nanoparticle Fillers. NP-filled CPEs have been most widely investigated. Pioneering work by Croce et al.[10] indicated a PEO-$LiClO_4$ solid electrolyte with TiO_2 and Al_2O_3 NPs, showing ionic conductivity of 10^{-4} S cm^{-1} at 50°C and 10^{-5} S cm^{-1} at 30°C, respectively. The SiO_2 NPs added with plasticizers proposed by Nan's group[73] also provide a promising approach to fabricating high-performance CPEs. However, there was no big breakthrough since 1998 until the development of nanotechnology, to which more and more researchers paid attention, thus accelerating the development of CPEs. Recently, Cui's group introduced an *in situ* synthesis technology to suppress the degree of PEO crystallinity, demonstrating high ionic conductivities (ranging from 10^{-4} S cm^{-1} to 10^{-5} S cm^{-1} at RT).[72] Through *in situ* hydrolysis, SiO_2 NPs with precise size and high monodispersity could enable a larger Lewis acid-base interaction surface area (green line in Figure 9). The crystallinity of PEO was also reduced by the monodispersed ultrafine SiO_2 spheres (Figure 10A), which results in an enhanced ionic conductivity.[72,101] For improvement of ionic conductivity, Li-ion-conducting nanofillers have been

Please cite this article in press as: Xia et al., Practical Challenges and Future Perspectives of All-Solid-State Lithium-Metal Batteries, Chem (2018), https://doi.org/10.1016/j.chempr.2018.11.013

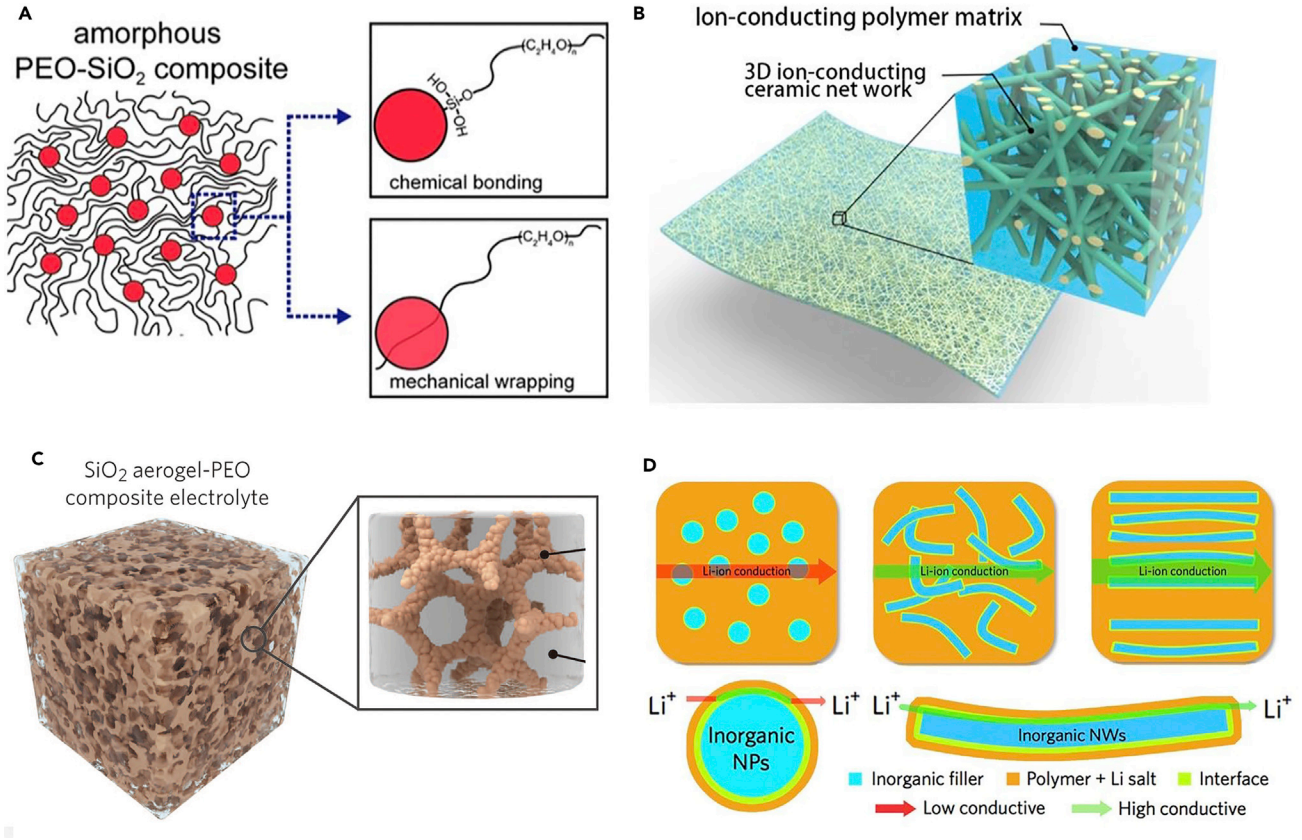

Figure 10. Schematics of CPEs with Fillers of Different Morphologies

(A) Schematic of PEO/MUSiO$_2$ NPs. Reprinted with permission from Lin et al.[72] Copyright 2016 American Chemical Society.

(B) Schematic of the 3D NWs network in CPE. Reprinted with permission from Fu et al.[108] Copyright 2016 National Academy of Sciences.

(C) Schematic of the SiO$_2$-aerogel-reinforced CPE. Reprinted with permission from Lin et al.[109] Copyright 2018 Wiley-VCH Verlag GmbH & Co. KGaA.

(D) The comparison of possible Li-ion-conduction pathways for CPEs with NPs, random NWs and aligned NWs. Reprinted with permission from Liu et al.[103] Copyright 2017 Springer Nature.

proposed. Recently, Zhang et al.[24] reported that the incorporation of Ta-LLZO NPs into a PVDF matrix could induce structural modification of polymer matrix, resulting in enhancement of the interaction of PVDF, Li salt, and Ta-LLZO fillers. As a result, the achieved CPEs showed improved properties such as an excellent ionic conductivity as high as 5×10^{-4} S cm^{-1} at RT (red line in Figure 9), good mechanical strength, and thermal stability.

Nanowire Fillers. Unlike NPs with particle-particle junctions, NWs can build a 3D network for fast Li-ion transportation, due to the continuous and extended hopping pathway on the NW surface. Cui's group first reported important work on CPEs, indicating that enhanced ionic conductivity and electrochemical stability could be achieved through the use of 1D nanofillers. Li-ion conductive LLTO NWs were originally synthesized by electrospinning. PAN-LiClO$_4$ CPE with LLTO NWs showed an extremely high ionic conductivity of 2.4×10^{-4} S cm^{-1} at RT, which is three orders of magnitude larger than the fill-free electrolyte (gray line in Figure 9).[11] Li-ion-conducting LLZO NWs were also used to improve the ionic conductivity of SPE (blue line in Figure 9).[104,108] Later, 7 mol % of Y$_2$O$_3$-doped ZrO$_2$ (7YSZ) NWs with positive-charged oxygen vacancies on surface were also used to help release free Li ions, resulting in a high ionic conductivity of 1.07×10^{-5} S cm^{-1} at 30°C (brown line in Figure 9).[110]

Please cite this article in press as: Xia et al., Practical Challenges and Future Perspectives of All-Solid-State Lithium-Metal Batteries, Chem (2018), https://doi.org/10.1016/j.chempr.2018.11.013

For uniformly dispersed NWs and NPs, junctions between fillers are considered one of the main hindrances to the high ionic conductivity, as illustrated in Figure 10D.[103,111] Most recently, the concept of aligned NPs and NWs has been introduced by some works to deal with this problem. Liu et al.[103] demonstrated that well vertically aligned LLTO NWs can significantly enhance the ionic conductivity of CPEs due to their long-range ionic conducting channels without obstructive cross-junctions (Figure 10D). A 10-fold improvement (6.05×10^{-5} S cm^{-1} at 30°C) compared with the randomly dispersed NWs has been observed (fuschia line in Figure 9). The aligned NWs also built a platform for us to deduce the surface conductivity of the nanofillers, which was 1.26×10^{-2} S cm^{-1} at 30°C. LTN appeared to be improved because more free Li ions were released as a result of the association between the NWs and the Li salt, whereas extended Li-ion hopping distance was achieved on the surfaces with more Li vacancy defects. Apparently, a fast ion-transport pathway on surfaces with no junctions is the main reason for the increased conductivity (Figure 10D).

Later, the ice-templating method was employed by Yang et al. to fabricate vertically aligned and connected LATP NPs,[111] which act as ion-conducting channels for Li ions, and filled this vertically aligned structure with PEO afterward. As the ice-templating process does not exert pressure on the electrolyte, this will lead to poor ionic conductivity at the particle-particle interface. Meanwhile, inserted PEO in the intervals between the particles may block the ion-conducting channels. To solve this issue, Yang et al. added polyethylene glycol (PEG) as a plasticizer to reduce the interfacial resistance, whereby the ionic conductivity of this LATP/PEO/PEG system with aligned NPs was 3.6-fold better than the same system with randomly dispersed NPs and reached 5.2×10^{-5} S cm^{-1}, close to its theoretical value (4.5×10^{-5} S cm^{-1}) (sky-blue line in Figure 9). Very recently, Fan's group[112] developed a PEO-based composite electrolyte reinforced with a 3D LATP/PAN fiber network, which delivered a stable cycling for 400 hr under a current density of 0.3 mA cm^{-2} for the Li symmetric cell.

Nanoplate Fillers. Two-dimensional (2D) mesoporous nanoplates such as montmorillonite,[113] clay,[114] and mica[115] are also promising candidates as fillers for high-performance CPEs. A CPE with 8 wt % polymerized ionic liquid functionalized mesoporous silica nanoplate showed an ionic conductivity of 1.8×10^{-5} S cm^{-1} at 20°C.[116] It is supposed that the improvement of ionic conductivity is due to the long-range ion-transport trajectory and the interconnection of the conductive channels at a 5–8 wt % loading. It is also reported that it has excellent electrochemical stability and compatibility with LFP electrode. The capacity of the battery is 115.9 mAh g^{-1} at 0.1 C and 102.4 mAh g^{-1} at 0.4 C at 60°C.

Hence, it is believed that both the composition and the nanostructure of inorganic fillers are important. Active fillers such as garnet oxide could participate in Li-ion conduction and thus directly contribute to the overall performance of the composites. On the other hand, the nanostructure of the inorganic fillers is also important. Generally, 1D nanostructure is superior to isolated NPs because of their continuous and extended Li^+ transport channels. Meanwhile, the interaction of inorganic fillers with polymer matrix and Li salt also plays an important role on the ionic conductivities of CPEs. That the composite polymer electrolyte based on Ta-LLZO NPs (Figure 9) showed the best performance is partially because of its electrolyte system, where the interaction of PVDF and Ta-LLZO contributed to its excellent performance although the fillers are NP-structured.

Please cite this article in press as: Xia et al., Practical Challenges and Future Perspectives of All-Solid-State Lithium-Metal Batteries, Chem (2018), https://doi.org/10.1016/j.chempr.2018.11.013

Composite Solid Electrolyte with Ceramic Matrix. Generally, inorganic electrolytes show higher ionic conductivity than SPEs, but with a more difficult processing. Therefore, the difference in the processing window between polymers and ceramics as well as the limited volume fraction of ceramics used to be considered a major obstacle to reach the desired properties of CSEs. To further utilize the Li-ion-conduction channels along NW surface, Yang et al. proposed a 3D nanofiber network providing a long-range Li-ion transport pathway.[104] A flexible CPE based on a 3D NW matrix prepared by electrospinning has been reported by Hu's group.[108] They prepared a CPE consisting of a 3D garnet LLZO NW network (Figure 10B) with PEO and Li salt filler. An ionic conductivity of 2.5×10^{-4} S cm^{-1} at RT was achieved (yellow line in Figure 9). The symmetric battery using this NW network reinforced CPE ran at a current density of 0.5 mA cm^{-2} for over 300 cycles. In addition, mesoporous SiO_2 aerogel was used as the backbone to provide continuous fast Li-ion-conduction pathway in CSEs (Figure 10C). Cui's group[109] successfully fabricated CPEs consisting of interconnected SiO_2 aerogel filled with PEO-based electrolyte, showing a high modulus of 0.43 GPa and a high ionic conductivity of 0.6 mS cm^{-1} at 30°C (dark line in Figure 9). The resultant Li|LFP cells exhibited a high specific capacity of 105 mAh g^{-1} at 0.4 C at a low temperature of 15°C. Another pioneering work[117] demonstrated a concept of "polymer-in-ceramic" CPE, with high volume fraction of ceramics containing $Li_{6.4}La_3Zr_{1.4}Ta_{0.6}O_{12}$ and PEO by hot-pressing without organic solvent. It showed an ionic conductivity higher than 10^{-4} S cm^{-1} at temperatures higher than 50°C with good flexibility and enhanced mechanical properties. It is supposed that the improvement in conductivity results from the alternative Li-ion-conduction pathway provided by Ta-LLZO.

To optimize the Li-ion-conduction pathway along a ceramic surface, vertically aligned inorganic matrix should be of benefit. Very recently, CSEs with vertically aligned and continuous ceramic and polymer interface were reported by Cui's group, showing an outstanding ionic conductivity of 5.82×10^{-4} S cm^{-1}, which is the highest level reported for CSEs to date.[118] The excellent performances could be ascribed to the densely packed, vertically aligned, and continuous polymer-ceramic interface formed in CSEs.

In addition to seeking advanced materials with high electrochemical performance, the battery community also paid attention to orienting toward large-scale manufacture.[119,120] Compared with the lab-scale dry mixing process for all-solid-state batteries, Lee et al.[120] proposed a solution-based casting process by using an appropriate binder and solvent, facilitating the homogeneous dispersion of active particles as well as good adhesion between electrode materials. More importantly, their process is easy to magnify for large-scale production. Their work greatly contributed to the mass production of ASSLBs with the solution-based roll-to-roll process.

ALL-SOLID-STATE BATTERIES BASED ON LITHIUM-METAL ANODES

The hot spot of research on Li metal adopted as the anode has been revived in recent years. Li metal is an ideal anode candidate for the next generation of high-energy-density batteries owing to its high theoretical specific capacity (3,860 mAh g^{-1}), lowest negative electrochemical potential (−3.040 V versus standard hydrogen electrode), and low density (0.59 g cm^{-3}). The utilization of Li-metal anodes could promote advanced batteries using high-energy chemistries, such as Li-S and Li-air batteries. However, Li-metal-based batteries have several challenges impeding their applications. For example, Li metal tends to inhomogeneously deposit in the Li dendrite form, which could penetrate the separator, causing thermal runaway

Please cite this article in press as: Xia et al., Practical Challenges and Future Perspectives of All-Solid-State Lithium-Metal Batteries, Chem (2018), https://doi.org/10.1016/j.chempr.2018.11.013

and battery failure. Meanwhile, the SEI layer spontaneously formed at the Li metal surface by consumption of electrolyte could aid the inhomogeneous nucleation and lead to low CE. Additionally, large-volume variation of Li-metal anodes upon the repeated deposition and dissolution cycles could lead to cracks in the SEI layer, exposing fresh Li underneath reacting with Li metal continuously. The enhanced Li-ion flux occurring at cracks as a result of the lower energy barrier for Li-ion transport could aggravate the non-uniform Li deposition. After continuous cycling, the repeated Li plating and stripping processes could produce a porous Li electrode and large amount of dead Li with a low CE. Various approaches including electrolyte additives,[121] artificial SEI layers,[52] and engineering interfacial layers and Li host[54,56] have been proposed to address the problems with Li-metal anodes. Among these resolutions, developing SSEs for LMBs is a promising approach to resolve these problems. SSEs could provide straightforward physical obstacles inhibiting Li dendrite propagation. Monroe and Newman[122] indicated that the shear modulus of solid electrolyte should be at least twice that of metallic Li (~4.2 GPa) to suppress the dendrite growth, and it has been reported that even the garnet-based electrolyte with high modulus could not suppress Li dendrite growth by penetrating through grain boundaries under current densities higher than 0.5 mA cm^{-2}.[123] In the following section, three types of advanced ASSLMBs based on SSEs and Li-metal anodes will be discussed in detail.

All-Solid-State Lithium-Metal Batteries with Lithium-Intercalation Compound Cathodes

The main challenges of SPEs in battery application are their relatively limited ionic conductivity at RT, low voltage window, and narrow operating temperatures. Crosslinking is one effective approach to improve both the ionic conductivity and mechanical strength of PEO-based electrolytes.[6] Solid-state sp^3 boron-based single-ion-conducting PEO-based polymer electrolyte membranes (S-BSMs) were also reported for ASSLMBs construction.[82] The weak association between Li ions and the sp^3 boron atoms contributed to the high Li-ion mobility, and the measured LTN number of S-BSMs was close to unity. The fabricated Li|S-BSMs|LFP ASSLMBs exhibited excellent cycling performance with a discharge capacity of over 100 mAh g^{-1} and good electrochemical cycling stability even at a temperature of 50°C below the melting point of PEO. Their development is an important step for constructing ASSLMBs operating at ambient temperatures in the future.

To improve the mechanical strength and electrochemical properties of SPEs, incorporating inorganic filler to construct CPEs is the most often applied method. Recently, Xu's group[124] reported a facile and versatile construction strategy to fabricate an ionic conductive network in the cathode and improve the interfacial contact of the electrolyte and electrode by employing a cohesive and highly conductive PEO-based CPE both in the cathode layer and at the interface of the electrolyte and anode, achieving a 3D ionic conductive network in the cathode layer and superior interfacial contact of the electrolyte and electrode. The resulting Li|LFP ASSLMBs present an ultra-long cycle life and high capacity with a reversible discharge capacity of 127.8 mAh g^{-1} after 1,000 cycles at 1 C and 60°C. Recently, Ban et al.[125] reported a PEO/LATP composite solid electrolyte for Li|LFP ASSLMBs, showing excellent capacity retention of 76.3% even after 500 cycles at 1 C and 80°C. Polycarbonate-based electrolytes are promising SPEs compared with conventional PEO-based electrolytes owing to their superior RT ionic conductivity, higher LTN, wider electrochemical stability window, and better compatibility with Li-metal anode.[126] Very recently, Tao's group[127] reported CPEs with $Mg_2B_2O_5$ NWs, showing a high ionic conductivity of 1.53×10^{-4} S cm^{-1} at 40°C (Figure 11). The Li|LFP cells

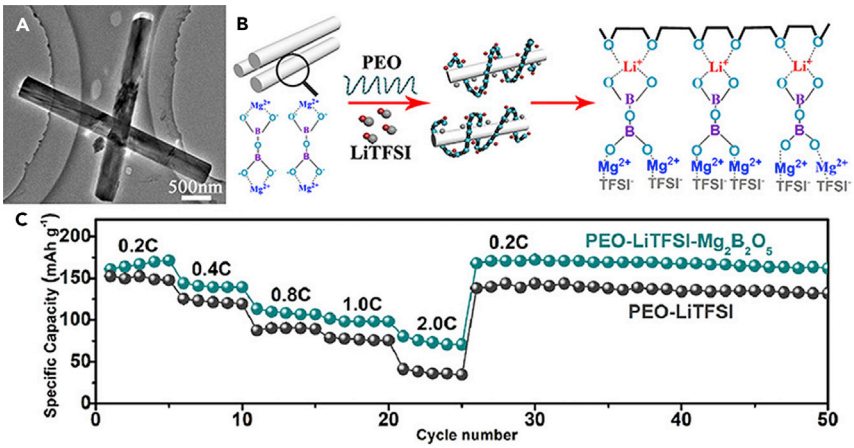

Figure 11. Morphology and Electrochemical Performances for CPEs with $Mg_2B_2O_5$ NWs
(A) TEM image of $Mg_2B_2O_5$ NWs.
(B) Schematic illustration of Li-ion conduction in CPEs with $Mg_2B_2O_5$ NWs.
(C) Rate performances of Li|LFP cells using SSEs with and without $Mg_2B_2O_5$ NWs at 50°C.
Reprinted with permission from Sheng et al.[127] Copyright 2018 American Chemical Society.

delivered a high specific capacity of 150, 106, and 50 mAh g^{-1} under 0.2 C at 50°C, 40°C, and 30°C, and a good cycling performance of specific capacity 120 mAh g^{-1} after 230 charge/discharge cycles under 1.0 C at 50°C.

However, PEO-based SPEs cannot be used with Li-intercalation cathode materials with a high voltage such as LCO, due to the low electrochemical stability. Adding ceramic nanofillers in SPEs is effective for improving the stability. Shen's group[24] reported high-performance flexible PVDF/Ta-LLZO CPEs for Li|LCO ASSLMBs. These batteries demonstrated a high RT discharge capacity of 150 mAh g^{-1}, and a capacity retention as high as 98% could be detected even after 120 cycles at 0.4 C. This CPE with high electrochemical performance showed great promise in ASSLMBs.

Inorganic SSEs are also applied in ASSLMBs. Lee's group[128] reported bendable inorganic Li|LiPON|LCO ASSLMBs showing an outstanding battery performance with a maximum specific capacity of 106 μAh cm^{-2} at RT, the highest performance for flexible LIBs at that time. Years later, Goodenough's group[129] reported a novel fluorine-doped anti-perovskite Li-ion conductor of $Li_2(OH)X$ (X = Cl, Br) with an outstanding electrochemical stability window as high as 9 V and excellent Li^+ conductivity. Based on this material, the obtained Li|LFP ASSLMBs showed an initial discharge capacity of 125 mAh g^{-1} at 0.2 C and 65°C with a high CE over 40 cycles. In the same year, they reported a stable rhombohedral structured NASICON-type $LiZr_2(PO_4)_3$ SSE with a bulk ionic conductivity of 2×10^{-4} S cm^{-1} and an electrochemical stability window as high as 5.5 V versus Li^+/Li.[46] A passivation layer of Li_8ZrO_6 and Li_3P formed as a result of the reaction of Li with $LiZr_2(PO_4)_3$ was not only wetted by Li metal but also prohibited the dendrite growth. Thus, this SSE showed a low interfacial resistance against both the Li-metal anode and the LFP cathode. The assembled Li|$LiZr_2(PO_4)_3$|LFP ASSLMBs thus showed good cycling stability with a discharge capacity of 140 mAh g^{-1} at the current density of 50 μA cm^{-2} at 80°C.

ASSLMBs also run well with the use of sulfide SSEs. In 2015, Xu and colleagues[130] reported new $75Li_2S \cdot (25-x)P_2S_5 \cdot xP_2O_5$ electrolytes (mol %) for fabricating a high-energy battery by using Li metal as a negative electrode. They found that the ionic conductivity of electrolyte could increase up to 56% with a 1 mol % P_2O_5

Please cite this article in press as: Xia et al., Practical Challenges and Future Perspectives of All-Solid-State Lithium-Metal Batteries, Chem (2018), https://doi.org/10.1016/j.chempr.2018.11.013

substitution, showing a high conductivity of 8×10^{-4} S cm^{-1} at RT. Moreover, the as-prepared $75Li_2S{\cdot}24P_2S_5{\cdot}P_2O_5$ electrolyte exhibited good stability and compatibility with the metallic Li anode, whereas the obtained Li|$75Li_2S{\cdot}24P_2S_5{\cdot}P_2O_5$|LCO ASSLMBs showed a discharge capacity of 109 mAh g^{-1} at 0.1 C and a high capacity retention of 85.2% after 30 cycles at RT. The excellent battery performance could be ascribed to their new interfacial design enabling intimate contact interface between electrolyte and active materials. Recently, Kanno's group[21] reported superionic conductors of $Li_{9.54}Si_{1.74}P_{1.44}S_{11.7}Cl_{0.3}$ and $Li_{9.6}P_3S_{12}$ demonstrating an outstanding ionic conductivity of 2.5×10^{-2} S cm^{-1} for $Li_{9.54}Si_{1.74}P_{1.44}S_{11.7}Cl_{0.3}$ and excellent high stability (~0 V versus Li metal) for $Li_{9.6}P_3S_{12}$. The obtained ASSLBs of LTO|$Li_{9.54}Si_{1.74}P_{1.44}S_{11.7}Cl_{0.3}$|LCO showed excellent rate performance 150 C and RT and even at 1,500 C and 100°C. In particular, the ASSLBs could exhibit excellent cycling performance at 100°C under a high current density of 18 C with ~75% capacity retention after 500 cycles (Figure 12A), whereas conventional LIBs with liquid electrolyte could not operate at so high a temperature because of the thermal instability of liquid electrolyte. For the fabricated ASSLMBs of Li|$Li_{9.6}P_3S_{12}$|LCO, an initial discharge capacity of over 100 mAh g^{-1} with a high CE of over 95% could be detected under the current density of 0.045 mA cm^{-2} at RT. Moreover, they investigated the electrochemical stability of the LGPS family against the Li metal via the initial charge and discharge efficiency data of Li|LGPS|LCO (Figure 12B). $Li_{9.6}P_3S_{12}$ in particular showed a high CE of 90%, indicating that $Li_{9.6}P_3S_{12}$ was quite stable with metallic Li, and almost all the Li ions from the cathode were deposited in the form of Li atom during the charging. In comparison, a low CE of only 61% was detected for the original LGPS, which means a large amount of Li was consumed due to the interfacial reaction resulting in an interfacial layer. The Ragone plots of energy density versus rate performance of the achieved batteries with previously reported batteries and capacitors are shown in Figure 12C. The achieved LTO|$LiNbO_3$-coated LCO ASSLBs showed remarkable and ultra-high electrical performances (E > 100 Wh kg^{-1}, P > 10 kW kg^{-1}), higher than conventional LIBs and supercapacitors, and even higher than advanced batteries.

SSEs with wide electrochemical window have the possibility of developing high-voltage cathode materials. However, the practical operation voltage of high-voltage cathode materials was usually higher than the electrochemical stability window of conventional carbonate-based liquid electrolyte (~4.3 V), inevitably resulting in electrolyte oxidative decomposition. Thus, low CE and limited cycle life were often observed for high-voltage cathode-based cells using liquid electrolytes.[22] Moreover, safety is another major challenge of high-voltage cathode-based Li batteries with flammable liquid electrolyte operating beyond their stable voltage limit. On the other hand, using SSEs could fundamentally circumvent the safety issues. In 2015, Dudney et al.[22] reported thin-film type ASSLMBs based on LiPON SSEs with high-voltage LNM cathode, demonstrating an outstanding cycling performance with 90% capacity retention even after 10,000 cycles and a CE as high as 99.98% at 5 C and RT. However, the loading of cathode material is low (~0.5 mg cm^{-2}). A bulk-type, solid-state high-voltage battery is urgently needed to meet the requirements of practical application.

Besides inorganic Li-compound cathode materials, polymeric materials also demonstrated good performances as electrodes in ASSLMBs. In 2014, Zhu et al.[131] successfully fabricated ASSLMBs based on organic pillar quinone ($C_{35}H_{20}O_{10}$) cathode and CPEs. The poly(methacrylate) (PMA)/PEG-$LiClO_4$/3 wt % SiO_2 CPE has an ionic conductivity as high 2.6×10^{-4} S cm^{-1} at RT. The pillar quinine cathode in ASSLMBs showed an average operation voltage of ~2.6 V and a high initial capacity of

Please cite this article in press as: Xia et al., Practical Challenges and Future Perspectives of All-Solid-State Lithium-Metal Batteries, Chem (2018), https://doi.org/10.1016/j.chempr.2018.11.013

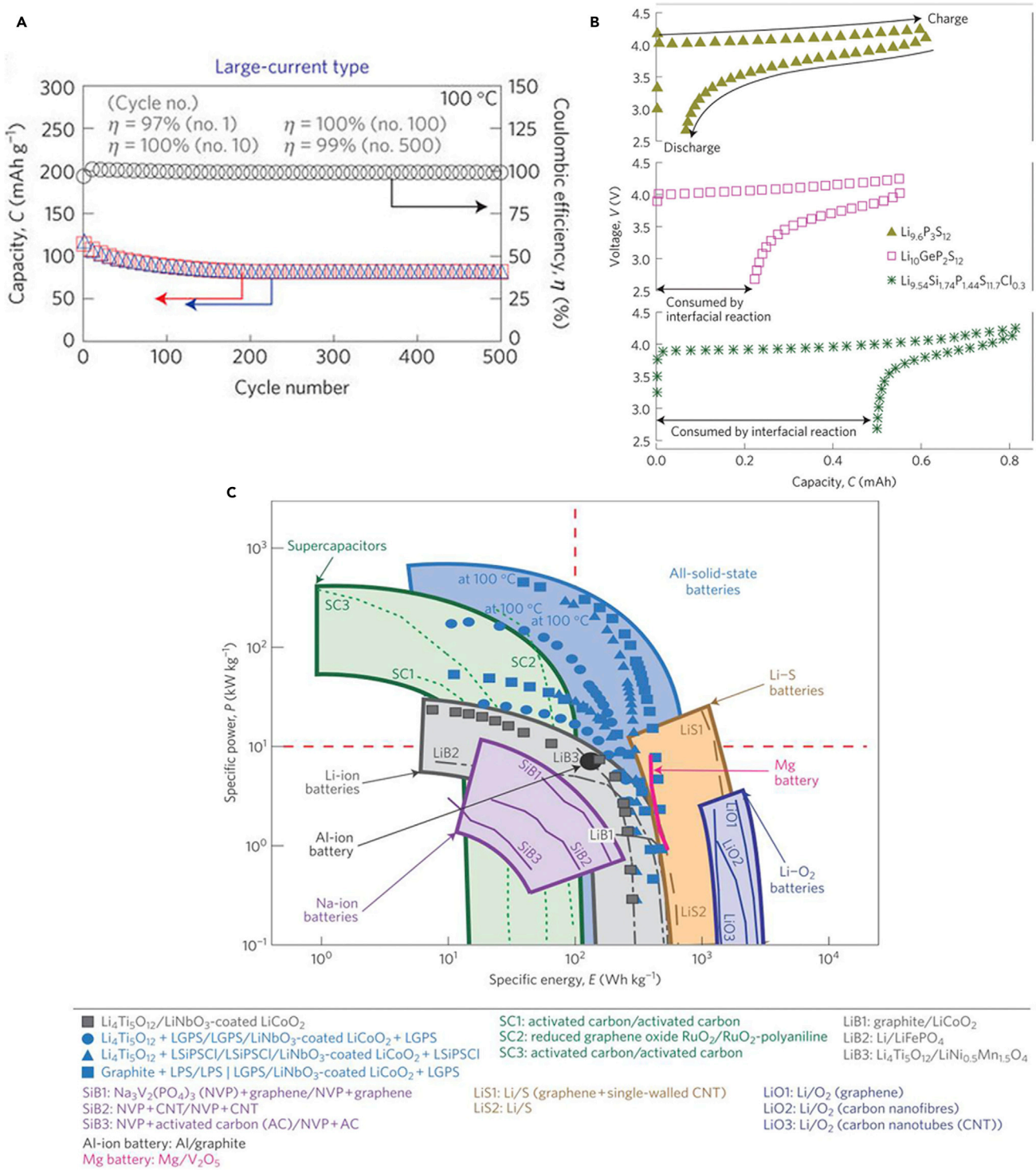

Figure 12. Electrochemical Performance of Electrolytes and Batteries

(A) Cycling performance of LTO|$Li_{9.54}Si_{1.74}P_{1.44}S_{11.7}Cl_{0.3}$|LCO ASSLBs at 18 C and 100°C.

(B) Electrochemical stability of the LGPS family.

(C) The Ragone plot of batteries. The red dashed line indicates the specific energy E = 100 Wh kg^{-1} and specific power P = 10 kW kg^{-1}.

Reprinted with permission from Kato et al.[21] Copyright 2016 Springer Nature.

Please cite this article in press as: Xia et al., Practical Challenges and Future Perspectives of All-Solid-State Lithium-Metal Batteries, Chem (2018), https://doi.org/10.1016/j.chempr.2018.11.013

418 mAh g^{-1} with a stable cyclability of 94.7% capacity retention after 50 cycles at 0.2 C through the reversible redox reactions of enolate and quinonid carbonyl groups, thus showing favorable application prospects for the device with high capacity.

Although the extremely high ionic conductivities of 10^{-3}–10^{-2} S cm^{-1} comparable with those of liquid electrolytes have been achieved in SSEs, the battery using such an SSE could not run as well, which is mainly attributed to the high interfacial resistance between electrolyte and electrode. To improve the Li^+ transfer at the electrolyte-electrode interface, Van Den Broek et al.[132] raised a new strategy of constructing porous garnet LLZO interface structure and fabricated a full-ceramic Li|LLZO|LTO ASSLMBs showing stable battery cycling performance. Their work demonstrated for the first time that ASSLMBs based on LLZO could cycle reversibly even at low potential and with ceramic anode material. Zhou et al.[133] constructed a polymer/ceramic-membrane/polymer sandwich electrolyte to improve the wettability of the LLZO ceramic pellet with Li-metal anode. The obtained Li|LFP ASSLMBs with the polymer interlayer showed a stable discharge specific capacity of 130 mAh g^{-1} even for 100 cycles at 65°C and 0.2 C. Co-fired electrolyte and electrode could result in a low interfacial resistance, as indicated by Ohta et al.[134] They successfully fabricated Li|LLZO|LCO ASSLMBs via the co-sintering technique, showing charge and discharge capacity of 98 and 78 mAh g^{-1}. Their work proved the feasibility of constructing ASSLBs by a simple co-sintering method. Very recently, Wang's group[25] reported all-ceramic Li|LLZO|LCO ASSLMBs with low interfacial resistance achieved via thermal soldering of cathode and electrolyte by the reaction of $Li_{2.3}C_{0.7}B_{0.3}O_3$ and Li_2CO_3. The obtained batteries showed excellent cycling stability and rate capability, which is the best performance to date for all-ceramic ASSLMBs. Thus, their work presented a significant breakthrough in developing ASSLMBs, demonstrating a promising prospect for the practical application of SSEs. The introduction of electrolytic salt in the cathode was also reported by Guo's group[135] to reduce the electrode-electrolyte interfacial resistance. The obtained Li|LFP ASSLMBs based on garnet $Li_{6.20}Ga_{0.30}La_{2.95}Rb_{0.05}Zr_2O_{12}$ (Ga-Rb-LLZO) exhibited an excellent initial specific capacity of 152 mAh g^{-1} and a capacity retention of 72.3% for the 20th cycle at 0.05 C and 60°C. Very recently, carbon post-treatment of LLZO solid electrolyte was reported by Li et al.,[136] which could remove the Li_2CO_3 and protons in the garnet framework and improve the wettability of LLZO with Li metal. The obtained Li|LFP ASSLMBs based on this kind of garnet showed an initial specific capacity of 143 mAh g^{-1} and a high capacity retention of 76.9% after the 40th cycle at 100 μA cm^{-2} and 65°C. In the same year, Liu et al.[137] reported garnet-type Ta-LLZO- for $Li|LiNi_{0.5}Co_{0.2}Mn_{0.3}O_2$ ASSLMB construction. It was found that the initial discharge specific capacity of the cells could increase from 112.7 to 123.3 mAh g^{-1} after surface modification of the cathode active materials with $Li[Ti_{0.1}Mn_{0.9}]_2O_4$ coating at a current density of 5 A cm^{-2} at 80°C.

All-Solid-State Lithium-Sulfur Batteries

Sulfur is considered a promising cathode candidate for next-generation high-energy systems owing to its high theoretical energy capacity (1,672 mAh g^{-1}), cost effectiveness, non-toxicity, and natural abundance.[138,139] However, some drawbacks prevent the commercialization of Li-S batteries, such as the low electronic and ionic conductivity of sulfur and sulfur-containing organic compounds and the Li polysulfide shuttle effect, leading to insufficient utilization of sulfur cathode.[139] The shuttle effect arises virtually from the dissolution and diffusion of polysulfide in organic liquid electrolyte. The polysulfides formed at the cathode can transport to Li anode where they are reduced to lower polysulfides, after which. the lower polysulfides can transport back

Please cite this article in press as: Xia et al., Practical Challenges and Future Perspectives of All-Solid-State Lithium-Metal Batteries, Chem (2018), https://doi.org/10.1016/j.chempr.2018.11.013

to the cathode where they are reoxidized before returning to the anode. The shuttle effect results in low active mass utilization, low CE and, thus, short cycling life.[138,139]

It should be noted that the electrochemical process is sensitive to the type of electrolytes in Li-S battery systems, which results in distinct reaction mechanisms and electrochemical characteristics when switching from liquid electrolytes to SSEs. Li-S batteries based on SSEs are promising ways to fundamentally solve the problem of soluble polysulfide in ether-based liquid electrolyte by effectively blocking the polysulfide diffusion by SSEs.[138] The first demonstration of solid-state Li-S battery was by DeGott in 1986, where a PEO-based electrolyte was adopted within the batteries cycling at 70°C. Later, three kinds of SPEs—PEO-based, poly(ethylene-methylene oxide) (PEMO)-based, and poly(ethylene glycol) dimethyl ether (PEGDME)-based polymer electrolytes—were studied with respect to the electrochemical performance of ASSLSBs.[140] However, these earlier ASSLSBs still faced the problems of low utilization of sulfur materials, serious capacity decay, and high operation temperatures. In 2010, Hassoun and Scrosati[141] reported high-performance ASSLSBs based on PEO-$LiCF_3SO_3$ matrix with nanosized ZrO_2 and Li_2S as electrolyte additives, which were new both in concept and composition. The dispersed ZrO_2 NPs not only improved the Li-ion transport of the polymer electrolyte in terms of ionic conductivity and LTN, but also stabilized the Li-metal-electrolyte interface. In the obtained ASSLSB, the specific capacity could reach a value of 900 mAh g^{-1} at 0.05 C, and the charge and discharge CE approached 100%, indicating the reduction of shuttle effect. Liang et al.[142] then applied the $PEO_{18}Li(CF_3SO_2)_2N/SiO_2$ electrolyte as a barrier to trap the polysulfides at the cathode side. They used ordered mesoporous carbon spheres as the conductive agent and held S in the channels of carbon spheres as the cathode to prepare the ASSLSBs. The obtained battery could retain a reversible discharge capacity of ~800 mAh g^{-1} after 25 cycles at 70°C with a current density of 0.1 mA cm^{-2}. Recently, Lin et al.[143] reported a novel natural nanosized halloysite filled PEO-based CPE with 3D ordered channels showing a high RT ionic conductivity of 1.11×10^{-4} S cm^{-1} (Figure 13A) for ASSLSB fabrication, demonstrating that the obtained batteries showed an average discharge capacity of 745 mAh g^{-1} after 100 discharge/charge cycles at 0.1 C and RT that could be applied in a wide temperature range of 25°C–100°C (Figures 13B and 13C). Recently, Cui's group[30] synthesized LLZO decorated porous carbon foam by sol-gel method and then used it as a matrix to hold S for constructing PEO-based composite S cathode material (Figure 13D). The S composite cathode based on PEO/LLZO composite solid electrolyte could deliver a high specific capacity of above 900 mAh g^{-1} for 200 cycles at 37°C under a current density of 0.05 mA cm^{-2}, showing stable cycling performance as well as high CE (Figure 13E).

Compared with polymeric SSEs, inorganic SSEs are promising candidates for ASSLSBs because of their high ionic conductivity at RT. Particularly, sulfide electrolytes that have similar chemical potential with sulfur or sulfide cathode materials could be the most promising SSE candidates for a rechargeable Li-S battery with lower interfacial resistance. Glass-type P_2S_5-Li_2S was used by Yamada and co-workers as SSE for ASSLSBs.[144] A high capacity of 1,600 mAh g^{-1} was achieved for the obtained ASSLSBs in the initial discharge-charge cycle with a high CE approaching 99%. Recently, Xu's group[145] reported high-performance ASSLSBs based on S-coated reduced graphene oxide (rGO) cathode with bilayered SSEs of LGPS/75%Li_2S-24%P_2S_5-1%P_2O_5. They deposited a 2-nm-thick layer of amorphous S on the rGO substrate to achieve high electronic conductivity and weaken the stress and strain of S composite cathode. The obtained ASSLSBs showed an outstanding initial discharge capacity of 1,629 mAh g^{-1} at 60°C under 0.02 C approaching the

Please cite this article in press as: Xia et al., Practical Challenges and Future Perspectives of All-Solid-State Lithium-Metal Batteries, Chem (2018), https://doi.org/10.1016/j.chempr.2018.11.013

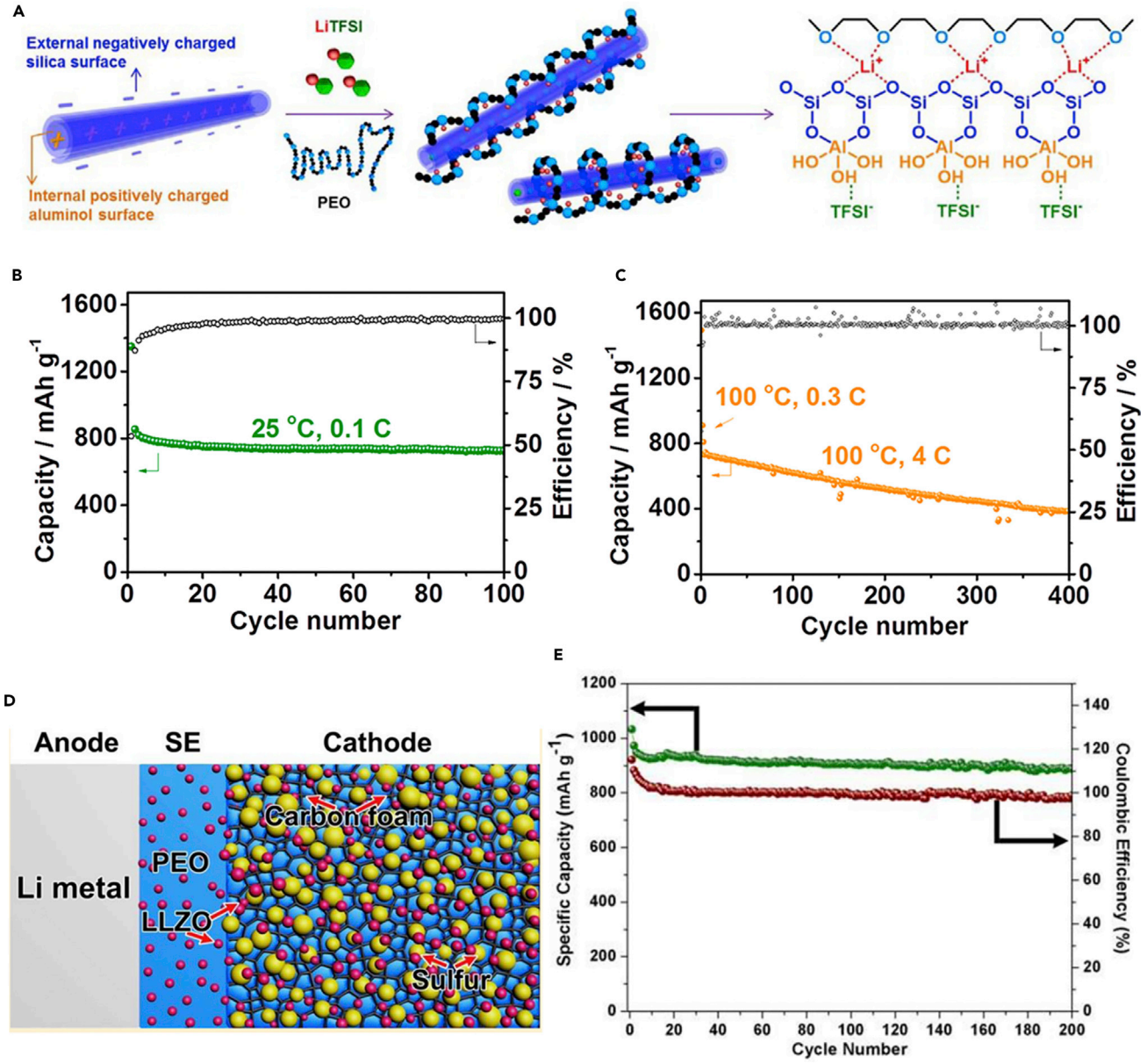

Figure 13. Schematics of CPEs, a CPE-Based Battery, and Their Corresponding Battery Cycling Performances

(A–C) Schematic showing the preparation method of HNT modified flexible PEO CPEs and mechanism of HNT addition for enhanced ionic conductivity (A) and cycling performances of the batteries at 25°C (B) and 100°C (C). Reprinted from Lin et al.[143]

(D and E) Schematic of ASSLSBs based on PEO/LLZO CPEs (D) and cycling performance and Coulombic efficiency of the S@LLZO@C cathode with a current density of 0.05 mA cm^{-2} at 37°C (E). Reprinted with permission from Tao et al.[30] Copyright 2017 American Chemical Society.

theoretical capacity of sulfur and rate performance as excellent as those with organic liquid electrolyte. Moreover, the batteries cycled stably for as many as 750 cycles with a reversible capacity of 830 mAh g^{-1} at 1 C and 60°C. The authors proposed that reducing the stress and strain of ASSLSBs could extend the battery cycling life. In the same year, a new SSE of MoS_2-tailored P_2S_5-Li_2S was reported by Tu's group[146] for constructing ASSLSBs. The doping of MoS_2 improved the stability of SSEs faced with Li-metal anode and the obtained electrolyte displayed a high RT conductivity of 4.8 × 10^{-3} S cm^{-1} and a wide electrochemical window as high as 5.0 V versus Li^+/Li. The assembled ASSLSBs based on the optimal electrolyte

Please cite this article in press as: Xia et al., Practical Challenges and Future Perspectives of All-Solid-State Lithium-Metal Batteries, Chem (2018), https://doi.org/10.1016/j.chempr.2018.11.013

displayed an improved high discharge capacity of 1,020 mAh g^{-1} and long cycling life under 0.05 C at RT. However, almost all SSEs are unstable with an Li-metal anode, requiring further investigation for real applications in ASSLMBs.[39,64]

All-Solid-State Lithium-Air Batteries

Li-air batteries (LABs) are fascinating devices deemed as a large-scale energy-storage technology due to their highest energy density (~11,140 Wh kg^{-1}) among various types of batteries.[34] The first non-aqueous rechargeable LAB was reported by Abraham and Jiang,[26] and the research interest has expanded rapidly in recent years. Nevertheless, the decomposition of organic liquid electrolyte leading to large polarization, capacity degradation, and safety concerns blocked the practical application of LABs. Developing SSEs based on LABs could fundamentally eliminate safety issues. Although ASSLABs have not yet been investigated extensively due to the very challenging problems such as large polarization resistance and quick capacity decay, together with the Li dendrite formation, a certain degree of success has been obtained.

Compared with inorganic electrolyte with high mechanical strength, polymeric electrolyte showed superior processability properties. In particular, CPEs composed of inorganic filler in the polymer matrix could show higher ionic conductivity and better mechanical strength while retaining relatively good processability. In 2011, ZrO_2-doped PEO-based CPEs were reported by Hassoun et al.[147] for the construction of ASSLABs. Their work demonstrated the viability of LABs based on CPEs, although underlying challenges arise from the large interfacial resistance. They also proposed a mechanism for oxidation of Li peroxides and reported multilayer structured CPEs of lamination of glass-ceramic (GC) and polymer-ceramic (PC) layers. Kumar et al.[31] fabricated ASSLABs consisting of a Li-metal anode, a solid electrolyte membrane laminated from GC and PC, and a composite air cathode prepared with carbon and GC powder. The achieved batteries were thermally stable and rechargeable in the temperature range of 30°C–105°C and could be subjected to 40 reversible charge-discharge cycles, with low polarization. Their work presented a major contribution to seeking an energy-storage system with ultra-high energy density. Zhou and colleagues[148] then reported a double-layer electrolyte composed of a PEO-based SPE layer facing Li metal and an LATP layer facing the air electrode for fabrication of ASSLABs. The polymer membrane layer incorporated could avoid the direct contact of LATP with Li-metal anode thus avoiding the reduction of Ti^{4+} by Li metal, whereas a large interfacial resistance inevitably formed at the interface between Li anode and the electrolyte. Their work pointed out that solid electrolyte without polymers will be a promising candidate for ASSLABs. Recently, Balaish et al.[149] also developed a PEO-based SPE for ASSLAB fabrication (Figure 14A).[32] The obtained batteries demonstrated an excellent electrochemical performance as high as that with liquid electrolyte of ethylene glycol dimethyl ether, showing reversible charge and discharge stability under the current density of 0.2 mA cm^{-2} at 80°C (Figure 14B) for 40 cycles. Their work proved that PEO-based SPEs are promising SSEs for fabricating high-performance ASSLABs.

Inorganic SSEs were also reported for ASSLABs. In 2012, Zhou and Kitaura[150] proposed the designs for ASSLABs using pure inorganic SSEs. They chose LAGP electrolyte due to its relatively high ionic conductivity and favorable chemical stability against Li-metal anode. The inorganic electrolyte was directly attached to the Li-metal anode. It demonstrated that the polarization issue was weakened in ASSLABs compared with those of liquid electrolyte. The initial discharge and charge capacities for the Li|LAGP|LAGP@CNT-air ASSLABs were 1,700 and

Please cite this article in press as: Xia et al., Practical Challenges and Future Perspectives of All-Solid-State Lithium-Metal Batteries, Chem (2018), https://doi.org/10.1016/j.chempr.2018.11.013

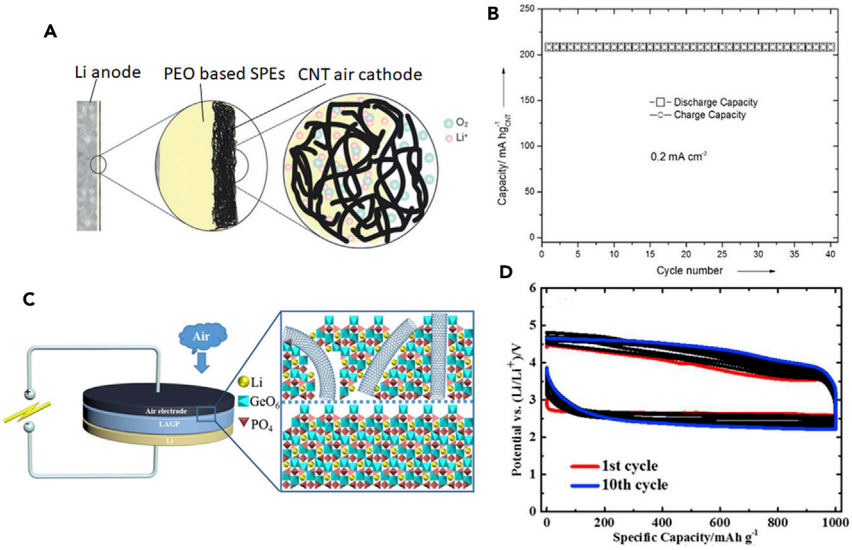

Figure 14. Schematics of ASSLABs and Their Corresponding Electrochemical Cycling Performances

(A and B) Schematic of PEO-based ASSLABs (A) and the cycling performance of ASSLABs at 0.2 mA cm^{-2} and 80°C (B). Reprinted with permission from Balaish et al.[149] Copyright 2015 Wiley-VCH Verlag GmbH & Co. KGaA.

(C and D) Schematic of ASSLABs with LAGP SSEs (C) and the cycling performance of the ASSLABs at 400 mA g^{-1} (D). Reprinted with permission from Liu et al.[32] Copyright 2015 American Chemical Society.

900 mAh g^{-1}, respectively under a current density of 900 mA g^{-1} with a voltage range of 2.0–4.2 V versus Li^+/Li. Recently, Zhou's group[32] fabricated a composite air electrode consisting of single-walled carbon nanotubes (SWCNTs) and LAGP (Figure 14C), showing higher capacity of 2,800 mAh g^{-1} compared with those with multi-walled carbon nanotube-LAGP cathode. Moreover, the obtained Li|LAGP|SWCNTs/LAGP/air ASSLABs demonstrated superior cycling performance with a reversible capacity of 1,000 mAh g^{-1} at the current density of 400 mA g^{-1} (Figure 14D), which could be ascribed to the large surface area and the good electronic conduction of SWCNTs.

CONCLUDING REMARKS AND FUTURE PERSPECTIVES

Accompanied by the development of high-capacity chemistries, such as Li-metal anodes and sulfur and oxygen cathode materials, SSEs are playing an increasingly significant role in "beyond Li" batteries with high energy density for large-scale energy-storage applications. The crucial problems with flammable organic liquid electrolytes and high-energy electrodes could be fundamentally resolved by the adoption of SSEs, including metallic Li dendrite growth with low CE, the shuttle effect of dissoluble polysulfide for sulfur cathode, and instability of battery components due to open surroundings of the air electrode. In this review, the current progress and challenges of SSEs during the past decades have been highlighted. Although many advances in SSEs have been achieved, there are still a few aspects to be mitigated before their successful practical implementation. Historically, through scientists' continuous efforts the ionic conductivities have been pushed up to over 10^{-3} S cm^{-1} in SSEs such as sulfide and garnet family, comparable with that of liquid electrolyte. However, most SSEs are ordinary double-dealers, meaning that these sulfides are unstable with Li metal or moisture, and the garnet-type oxides

Please cite this article in press as: Xia et al., Practical Challenges and Future Perspectives of All-Solid-State Lithium-Metal Batteries, Chem (2018), https://doi.org/10.1016/j.chempr.2018.11.013

Table 1. Electrochemical Performances of Recently Reported Representative ASSLMBs Based on Li-Metal Anodes

Year	ASSLMBs	Operation Conditions	Specific Capacity (mAh g^{-1})	Capacity Retention
2015	Li|75Li_2S•24P_2S_5•P_2O_5|LCO[130]	RT, 0.1 C	109	85.2%, cycle 30
2015	Li|LAGP|SWCNTs/LAGP/air[32]	400 mA g^{-1}	1,000	not available
2016	Li|copolymer|LFP[75]	60°C, 0.2 C	161.7	90.6%, cycle 100
2016	Li|polymer/LLZO/polymer|LFP[133]	65°C, 0.2 C	130	100%, cycle 100
2016	Li|LGPS|$LiNi_{0.5}Mn_{1.5}O_4$[23]	RT, 0.1 C	80	71.3%, cycle 10
2017	Li|PEO/75Li_2S•24P_2S_5•1%P_2O_5/LAGP|LFP[124]	60°C, 0.1 C	153.4	99.9%, cycle 200
2017	Li|PVDF/Ta-LLZO|LCO[24]	RT, 0.4 C	150	98%, cycle 120
2017	Li|75Li_2S•24P_2S_5•1%P_2O_5/LGPS|rGO@S[145]	60°C, 1 C	903.2	91.8%, cycle 750
2017	Li|PEO/LLZO|S@LLZO@C[30]	37°C, 0.05 mA cm^{-2}	>900	98.7%, cycle 90
2017	Li|Ga-Rb-LLZO|LFP[135]	60°C, 0.05 C	152	72.3%, cycle 20
2018	Li|LLZO|LCO[25]	100°C, 0.05 C	144	46.5%, cycle 40
2018	Li|Ta-LLZO|$LiNi_{0.5}Co_{0.2}Mn_{0.3}O_2$[137]	80°C, 5 A cm^{-2}	123.3	62.1%, cycle 50
2018	Li|PEO/LATP|LFP[125]	80°C, 1 C	143.2	76.3%, cycle 500

RT, room temperature.

are not recommended due to high-temperature fabrication processing and their brittle features. In recent years, the poor kinetic and thermodynamic stability at the electrolyte-electrode interfaces have attracted much more attention with regard to full cells. Continuous achievements on the reduction of interface impedances, such as composite electrodes with electrolyte additives, artificial SEI layers, and interfacial modifications, have been discussed in this review. Additionally and subsequently, the current progress of ASSLMBs based on Li-metal anodes coupled with Li-intercalation-compound, sulfur, and oxygen cathodes listed in Table 1 have also been discussed, revealing the initial accomplishments and the many challenges remaining to be addressed.

SSEs are showing increasingly attractive prospects and potential in next-generation batteries. Scientists and engineers still need to devote efforts to the development of commercially competitive SSEs in terms of ionic conductivity, interfacial impedances, mechanical strength, and compatibility with electrodes while at an affordable cost. It should be noted that different advantages should be effectively utilized according to different applications, such as high power density for portable electronics and electric vehicles and low maintenance cost for smart grid storage, besides the required high energy density. Exploration of new techniques such as optimizing the battery design structure to improve the overall performances is also imperative. Moreover, modifying the existing battery fabrication processes or reinventing new manufacturing technologies for ASSLMBs is important for short-term practical applications. As the saying goes, the road is tough and long, but the destination is eventually approached. ASSLMBs providing high energy density as well as high power density, long cycle life, and high degree of safety will move from infancy to maturity toward the ultimate battery in the future.

ACKNOWLEDGMENTS

The authors gratefully acknowledge financial support from ShanghaiTech University start-up funding, the 1,000 Young Talent Program, the National Natural Science Foundation of China (grant 21805185), the Shanghai Sailing Program (18YF1416800), and the China Postdoctoral Science Foundation (2017M621574).

Please cite this article in press as: Xia et al., Practical Challenges and Future Perspectives of All-Solid-State Lithium-Metal Batteries, Chem (2018), https://doi.org/10.1016/j.chempr.2018.11.013

REFERENCES AND NOTES

1. Haering, R.R., Stiles, J.A.R., and Brandt, K. (1980). US Patent 4224390A, filed August 30, 1979, and granted September 23, 1980.
2. Whittingham, M.S. (2004). Lithium batteries and cathode materials. Chem. Rev. *104*, 4271–4302.
3. Nagaura, T. (1990). Lithium ion rechargeable battery. Prog. Batteries Solar Cells *9*, 209–217.
4. Lin, D., Liu, Y., and Cui, Y. (2017). Reviving the lithium metal anode for high-energy batteries. Nat. Nanotechnol. *12*, 194–206.
5. Wang, Q., Song, W.L., Wang, L., Song, Y., Shi, Q., and Fan, L.Z. (2014). Electrospun polyimide-based fiber membranes as polymer electrolytes for lithium-ion batteries. Electrochim. Acta *132*, 538–544.
6. Zhou, D., Fan, L.Z., Fan, H., and Shi, Q. (2013). Electrochemical performance of trimethylolpropane trimethylacrylate-based gel polymer electrolyte prepared by in situ thermal polymerization. Electrochim. Acta *89*, 334–338.
7. Chen, Z., Hsu, P.C., Lopez, J., Li, Y., To, J.W., Liu, N., Wang, C., Andrews, S.C., Liu, J., and Cui, Y. (2016). Fast and reversible thermoresponsive polymer switching materials for safer batteries. Nat. Energy *1*, https://doi.org/10.1038/nenergy.2015.9.
8. Fenton, D.E., Parker, J.M., and Wright, P.V. (1973). Complexes of alkali metal ions with poly (ethylene oxide). Polymer *14*, 589, https://doi.org/10.1016/0032-3861(73)90146-8.
9. Armand, M., Chabagno, J., and Duclot, M. (1979). Poly-ethers as solid electrolytes. In Fast Ion Transport in Solids: Electrodes and Electrolytes, P. Vashishta, J.N. Mundy, and G.K. Shenoy, eds. (Elsevier), p. 131.
10. Croce, F., Appetecchi, G.B., Persi, L., and Scrosati, B. (1998). Nanocomposite polymer electrolytes for lithium batteries. Nature *394*, 456–458.
11. Liu, W., Liu, N., Sun, J., Hsu, P.C., Li, Y., Lee, H.W., and Cui, Y. (2015). Ionic conductivity enhancement of polymer electrolytes with ceramic nanowire fillers. Nano Lett. *15*, 2740–2745.
12. Masdupuy, E. (1957). Ann. Chim. (Paris) *13*, 527–586.
13. Bates, J.B., Dudney, N.J., Gruzalski, G.R., Zuhr, R.A., Choudhury, A., Luck, C.F., and Robertson, J.D. (1992). Electrical properties of amorphous lithium electrolyte thin films. Solid State Ion. *53-56*, 647–654.
14. Dudney, N.J., Bates, J.B., Zuhr, R.A., Luck, C.F., and Robertson, J.D. (1992). Sputtering of lithium compounds for preparation of electrolyte thin films. Solid State Ion. *53-56*, 655–661.
15. Inaguma, Y., Liquan, C., Itoh, M., Nakamura, T., Uchida, T., Ikuta, H., and Wakihara, M. (1993). High ionic conductivity in lithium lanthanum titanate. Solid State Commun. *86*, 689–693.
16. Fu, J. (1997). Fast Li^+ ion conducting glass-ceramics in the system Li_2O-Al_2O_3-GeO_2-P_2O_5. Solid State Ion. *104*, 191–194.
17. Fu, J. (1997). Superionic conductivity of glass-ceramics in the system Li_2O-Al_2O_3-TiO_2-P_2O_5. Solid State Ion. *96*, 195–200.
18. Murugan, R., Thangadurai, V., and Weppner, W. (2007). Fast lithium ion conduction in garnet-type $Li_7La_3Zr_2O_{12}$. Angew. Chem. Int. Ed. *46*, 7778–7781.
19. Kamaya, N., Homma, K., Yamakawa, Y., Hirayama, M., Kanno, R., Yonemura, M., Kamiyama, T., Kato, Y., Hama, S., Kawamoto, K., et al. (2011). A lithium superionic conductor. Nat. Mater. *10*, 682–686.
20. Seino, Y., Ota, T., Takada, K., Hayashi, A., and Tatsumisago, M. (2014). A sulphide lithium super ion conductor is superior to liquid ion conductors for use in rechargeable batteries. Energy Environ. Sci. *7*, 627–631.
21. Kato, Y., Hori, S., Saito, T., Suzuki, K., Hirayama, M., Mitsui, A., Yonemura, M., Iba, H., and Kanno, R. (2016). High-power all-solid-state batteries using sulfide superionic conductors. Nat. Energy *1*, https://doi.org/10.1038/nenergy.2016.30.
22. Li, J., Ma, C., Chi, M., Liang, C., and Dudney, N.J. (2015). Solid electrolyte: the key for high-voltage lithium batteries. Adv. Energy Mater. *5*, 1401408.
23. Oh, G., Hirayama, M., Kwon, O., Suzuki, K., and Kanno, R. (2016). Bulk-type all solid-state batteries with 5 V class $LiNi_{0.5}Mn_{1.5}O_4$ cathode and $Li_{10}GeP_2S_{12}$ solid electrolyte. Chem. Mater. *28*, 2634–2640.
24. Zhang, X., Liu, T., Zhang, S., Huang, X., Xu, B., Lin, Y., Xu, B., Li, L., Nan, C.W., and Shen, Y. (2017). Synergistic coupling between $Li_{6.75}La_3Zr_{1.75}Ta_{0.25}O_{12}$ and Poly(vinylidene fluoride) induces high ionic conductivity, mechanical strength, and thermal stability of solid composite electrolytes. J. Am. Chem. Soc. *139*, 13779–13785.
25. Han, F., Yue, J., Chen, C., Zhao, N., Fan, X., Ma, Z., Gao, T., Wang, F., Guo, X., and Wang, C. (2018). Interphase engineering enabled all-ceramic lithium battery. Joule *2*, 497–508.
26. Abraham, K., and Jiang, Z. (1996). A polymer electrolyte-based rechargeable lithium/oxygen battery. J. Electrochem. Soc. *143*, 1–5.
27. Ogasawara, T., Débart, A., Holzapfel, M., Novák, P., and Bruce, P.G. (2006). Rechargeable Li_2O_2 electrode for lithium batteries. J. Am. Chem. Soc. *128*, 1390–1393.
28. Degott, P. (1986). Polymère Carbone-Soufre: Synthèse et Propriétés Électrochimiques (Institut National Polytechnique de Grenoble).
29. Hayashi, A., Ohtomo, T., Mizuno, F., Tadanaga, K., and Tatsumisago, M. (2003). All-solid-state Li/S batteries with highly conductive glass-ceramic electrolytes. Electrochem. Commun. *5*, 701–705.
30. Tao, X., Liu, Y., Liu, W., Zhou, G., Zhao, J., Lin, D., Zu, C., Sheng, O., Zhang, W., Lee, H.W., et al. (2017). Solid-state lithium–sulfur batteries operated at 37°C with composites of nanostructured $Li_7La_3Zr_2O_{12}$/carbon foam and polymer. Nano Lett. *17*, 2967–2972.
31. Kumar, B., Kumar, J., Leese, R., Fellner, J.P., Rodrigues, S.J., and Abraham, K.M. (2010). A solid-state, rechargeable, long cycle life lithium-air battery. J. Electrochem. Soc. *157*, A50–A54.
32. Liu, Y., Li, B., Kitaura, H., Zhang, X., Han, M., He, P., and Zhou, H. (2015). Fabrication and performance of all-solid-state Li-air battery with SWCNTs/LAGP cathode. ACS Appl. Mater. Interfaces *7*, 17307–17310.
33. Ratner, M.A., Johansson, P., and Shriver, D.F. (2000). Polymer electrolytes: ionic transport mechanisms and relaxation coupling. MRS Bull. *25*, 31–37.
34. Quartarone, E., and Mustarelli, P. (2011). Electrolytes for solid-state lithium rechargeable batteries: recent advances and perspectives. Chem. Soc. Rev. *40*, 2525–2540.
35. Meyer, W.H. (1998). Polymer electrolytes for lithium-ion batteries. Adv. Mater. *10*, 439–448.
36. MacGlashan, G.S., Andreev, Y.G., and Bruce, P.G. (1999). Structure of the polymer electrolyte poly(ethylene oxide)$_6$:$LiAsF_6$. Nature *398*, 792–794.
37. Manthiram, A., Yu, X., and Wang, S. (2017). Lithium battery chemistries enabled by solid-state electrolytes. Nat. Rev. Mater. *2*, https://doi.org/10.1038/natrevmats.2016.103.
38. Maier, J. (2005). Nanoionics: ion transport and electrochemical storage in confined systems. Nat. Mater. *4*, 805–815.
39. Richards, W.D., Miara, L.J., Wang, Y., Kim, J.C., and Ceder, G. (2016). Interface stability in solid-state batteries. Chem. Mater. *28*, 266–273.
40. Maier, J. (1995). Ionic conduction in space charge regions. Prog. Solid State Chem. *23*, 171–263.
41. Schwöbel, A., Hausbrand, R., and Jaegermann, W. (2015). Interface reactions between LiPON and lithium studied by in-situ X-ray photoemission. Solid State Ion. *273*, 51–54.
42. Ohta, N., Takada, K., Zhang, L., Ma, R., Osada, M., and Sasaki, T. (2006). Enhancement of the high-rate capability of solid-state lithium batteries by nanoscale interfacial modification. Adv. Mater. *18*, 2226–2229.
43. Haruyama, J., Sodeyama, K., Han, L., Takada, K., and Tateyama, Y. (2014). Space-charge layer effect at interface between oxide cathode and sulfide electrolyte in all-solid-state lithium-ion battery. Chem. Mater. *26*, 4248–4255.
44. Woo, J.H., Trevey, J.E., Cavanagh, A.S., Choi, Y.S., Kim, S.C., George, S.M., Oh, K.H., and Lee, S.H. (2012). Nanoscale interface modification of $LiCoO_2$ by Al_2O_3 atomic layer deposition for solid-state Li batteries. J. Electrochem. Soc. *159*, A1120–A1124.
45. Kitaura, H., Hayashi, A., Ohtomo, T., Hama, S., and Tatsumisago, M. (2011). Fabrication of

electrode-electrolyte interfaces in all-solid-state rechargeable lithium batteries by using a supercooled liquid state of the glassy electrolytes. J. Mater. Chem. *21*, 118–124.

46. Li, Y., Zhou, W., Chen, X., Lü, X., Cui, Z., Xin, S., Xue, L., Jia, Q., and Goodenough, J.B. (2016). Mastering the interface for advanced all-solid-state lithium rechargeable batteries. Proc. Natl. Acad. Sci. U S A *113*, 13313–13317.

47. Hayashi, A., Nishio, Y., Kitaura, H., and Tatsumisago, M. (2008). Novel technique to form electrode-electrolyte nanointerface in all-solid-state rechargeable lithium batteries. Electrochem. Commun. *10*, 1860–1863.

48. Aso, K., Sakuda, A., Hayashi, A., and Tatsumisago, M. (2013). All-solid-state lithium secondary batteries using NiS-carbon fiber composite electrodes coated with Li_2S-P_2S_5 solid electrolytes by pulsed laser deposition. ACS Appl. Mater. Interfaces *5*, 686–690.

49. Han, F., Gao, T., Zhu, Y., Gaskell, K.J., and Wang, C. (2015). A battery made from a single material. Adv. Mater. *27*, 3473–3483.

50. Kato, A., Hayashi, A., and Tatsumisago, M. (2016). Enhancing utilization of lithium metal electrodes in all-solid-state batteries by interface modification with gold thin films. J. Power Sources *309*, 27–32.

51. Luo, W., Gong, Y.H., Zhu, Y.Z., Li, Y.J., Yao, Y.G., Zhang, Y., Fu, K., Pastel, G., Lin, C.F., Mo, Y.F., et al. (2017). Reducing interfacial resistance between garnet-structured solid-state electrolyte and Li-metal anode by a germanium layer. Adv. Mater. *29*, 1606042.

52. Fu, K.K., Gong, Y.H., Liu, B.Y., Zhu, Y.Z., Xu, S.M., Yao, Y.G., Luo, W., Wang, C.W., Lacey, S.D., Dai, J.Q., et al. (2017). Toward garnet electrolyte-based Li metal batteries: an ultrathin, highly effective, artificial solid-state electrolyte/metallic Li interface. Sci. Adv. *3*, e1601659.

53. Han, X., Gong, Y., Fu, K., He, X., Hitz, G.T., Dai, J., Pearse, A., Liu, B., Wang, H., Rubloff, G., et al. (2017). Negating interfacial impedance in garnet-based solid-state Li metal batteries. Nat. Mater. *16*, 572–579.

54. Wang, C., Gong, Y., Liu, B., Fu, K., Yao, Y., Hitz, E., Li, Y., Dai, J., Xu, S., and Luo, W. (2016). Conformal, nanoscale ZnO surface modification of garnet-based solid-state electrolyte for lithium metal anodes. Nano Lett. *17*, 565–571.

55. Luo, W., Gong, Y.H., Zhu, Y.Z., Fu, K.K., Dai, J.Q., Lacey, S.D., Wang, C.W., Liu, B.Y., Han, X.G., Mo, Y.F., et al. (2016). Transition from superlithiophobicity to superlithiophilicity of garnet solid-state electrolyte. J. Am. Chem. Soc. *138*, 12258–12262.

56. Fu, K., Gong, Y., Hitz, G.T., McOwen, D.W., Li, Y., Xu, S., Wen, Y., Zhang, L., Wang, C., Pastel, G., et al. (2017). Three-dimensional bilayer garnet solid electrolyte based high energy density lithium metal-sulfur batteries. Energy Environ. Sci. *10*, 1568–1575.

57. Yamamoto, K., Yoshida, R., Sato, T., Matsumoto, H., Kurobe, H., Hamanaka, T., Kato, T., Iriyama, Y., and Hirayama, T. (2014). Nano-scale simultaneous observation of Li-concentration profile and Ti-, O electronic structure changes in an all-solid-state Li-ion battery by spatially-resolved electron energy-loss spectroscopy. J. Power Sources *266*, 414–421.

58. Liu, Y., Lin, D., Jin, Y., Liu, K., Tao, X., Zhang, Q., Zhang, X., and Cui, Y. (2017). Transforming from planar to three-dimensional lithium with flowable interphase for solid lithium metal batteries. Sci. Adv. *3*, eaao0713.

59. Yang, C., Zhang, L., Liu, B., Xu, S., Hamann, T., McOwen, D., Dai, J., Luo, W., Gong, Y., Wachsman, E.D., et al. (2018). Continuous plating/stripping behavior of solid-state lithium metal anode in a 3D ion-conductive framework. Proc. Natl. Acad. Sci. U S A. *115*, 3770–3775.

60. Brazier, A., Dupont, L., Dantras-Laffont, L., Kuwata, N., Kawamura, J., and Tarascon, J.M. (2008). First cross-section observation of an all solid-state lithium-ion "nanobattery" by transmission electron microscopy. Chem. Mater. *20*, 2352–2359.

61. Sakuda, A., Hayashi, A., and Tatsumisago, M. (2010). Interfacial observation between $LiCoO_2$ electrode and Li_2S-P_2S_5 solid electrolytes of all-solid-state lithium secondary batteries using transmission electron microscopy. Chem. Mater. *22*, 949–956.

62. Kato, T., Hamanaka, T., Yamamoto, K., Hirayama, T., Sagane, F., Motoyama, M., and Iriyama, Y. (2014). In-situ $Li_7La_3Zr_2O_{12}$/$LiCoO_2$ interface modification for advanced all-solid-state battery. J. Power Sources *260*, 292–298.

63. Wang, Z., Santhanagopalan, D., Zhang, W., Wang, F., Xin, H.L., He, K., Li, J., Dudney, N., and Meng, Y.S. (2016). In situ STEM-EELS observation of nanoscale interfacial phenomena in all-solid-state batteries. Nano Lett. *16*, 3760–3767.

64. Yamamoto, K., Iriyama, Y., Asaka, T., Hirayama, T., Fujita, H., Fisher, C.A., Nonaka, K., Sugita, Y., and Ogumi, Z. (2010). Dynamic visualization of the electric potential in an all-solid-state rechargeable lithium battery. Angew. Chem. Int. Ed. *49*, 4414–4417.

65. Lim, J., Li, Y., Alsem, D.H., So, H., Lee, S.C., Bai, P., Cogswell, D.A., Liu, X., Jin, N., Yu, Y., et al. (2016). Origin and hysteresis of lithium compositional spatiodynamics within battery primary particles. Science *353*, 566–571.

66. Li, Y., Li, Y., Pei, A., Yan, K., Sun, Y., Wu, C.L., Joubert, L.M., Chin, R., Koh, A.L., Yu, Y., et al. (2017). Atomic structure of sensitive battery materials and interfaces revealed by cryo-electron microscopy. Science *358*, 506–510.

67. Khurana, R., Schaefer, J.L., Archer, L.A., and Coates, G.W. (2014). Suppression of lithium dendrite growth using cross-linked polyethylene/poly(ethylene oxide) electrolytes: a new approach for practical lithium-metal polymer batteries. J. Am. Chem. Soc. *136*, 7395–7402.

68. Gopalan, A.I., Santhosh, P., Manesh, K.M., Nho, J.H., Kim, S.H., Hwang, C.-G., and Lee, K.-P. (2008). Development of electrospun PVdF-PAN membrane-based polymer electrolytes for lithium batteries. J. Membr. Sci. *325*, 683–690.

69. Appetecchi, G.B., Croce, F., and Scrosati, B. (1995). Kinetics and stability of the lithium electrode in poly(methylmethacrylate)-based gel electrolytes. Electrochim. Acta *40*, 991–997.

70. Tominaga, Y., and Yamazaki, K. (2014). Fast Li-ion conduction in poly (ethylene carbonate)-based electrolytes and composites filled with TiO_2 nanoparticles. Chem. Commun. (Camb.) *50*, 4448–4450.

71. Zhang, J., Zhao, J., Yue, L., Wang, Q., Chai, J., Liu, Z., Zhou, X., Li, H., Guo, Y., and Cui, G. (2015). Safety-reinforced poly (propylene carbonate)-based all-solid-state polymer electrolyte for ambient-temperature solid polymer lithium batteries. Adv. Energy Mater. *5*, 1501082.

72. Lin, D.C., Liu, W., Liu, Y.Y., Lee, H.R., Hsu, P.C., Liu, K., and Cui, Y. (2016). High ionic conductivity of composite solid polymer electrolyte via in situ synthesis of monodispersed SiO_2 nanospheres in poly(ethylene oxide). Nano Lett. *16*, 459–465.

73. Nan, C.W., Fan, L., Lin, Y., and Cai, Q. (2003). Enhanced ionic conductivity of polymer electrolytes containing nanocomposite SiO_2 particles. Phys. Rev. Lett. *91* (26 Pt 1), 266104.

74. Choi, B., Kim, Y., and Shin, H. (2000). Ionic conduction in PEO-PAN blend polymer electrolytes. Electrochim. Acta *45*, 1371–1374.

75. Chen, B., Xu, Q., Huang, Z., Zhao, Y.R., Chen, S.J., and Xu, X.X. (2016). One-pot preparation of new copolymer electrolytes with tunable network structure for all-solid-state lithium battery. J. Power Sources *331*, 322–331.

76. Yuan, C., Li, J., Han, P., Lai, Y., Zhang, Z., and Liu, J. (2013). Enhanced electrochemical performance of poly (ethylene oxide) based composite polymer electrolyte by incorporation of nano-sized metal-organic framework. J. Power Sources *240*, 653–658.

77. Chen, L., Liu, Y., and Fan, L.Z. (2017). Enhanced interface stability of polymer electrolytes using organic cage-type cucurbit [6] uril for lithium metal batteries. J. Electrochem. Soc. *164*, A1834–A1840.

78. Ghosh, A., Wang, C., and Kofinas, P. (2010). Block copolymer solid battery electrolyte with high Li-ion transference number. J. Electrochem. Soc. *157*, A846–A849.

79. Sun, X.G., and Kerr, J.B. (2006). Synthesis and characterization of network single ion conductors based on comb-branched polyepoxide ethers and lithium bis(allylmalonato)borate. Macromolecules *39*, 362–372.

80. Bouchet, R., Maria, S., Meziane, R., Aboulaich, A., Lienafa, L., Bonnet, J.P., Phan, T.N.T., Bertin, D., Gigmes, D., Devaux, D., et al. (2013). Single-ion BAB triblock copolymers as highly efficient electrolytes for lithium-metal batteries. Nat. Mater. *12*, 452–457.

81. Ma, Q., Zhang, H., Zhou, C., Zheng, L., Cheng, P., Nie, J., Feng, W., Hu, Y.-S., Li, H., Huang, X., et al. (2016). Single lithium-ion conducting polymer electrolytes based on a super-delocalized polyanion. Angew. Chem. Int. Ed. *55*, 2521–2525.

82. Zhang, Y.F., Cai, W.W., Rohan, R., Pan, M.Z., Liu, Y., Liu, X.P., Li, C.C., Sun, Y.B., and Cheng, H.S. (2016). Toward ambient temperature

operation with all-solid-state lithium metal batteries with a sp^3 boron-based solid single ion conducting polymer electrolyte. J. Power Sources *306*, 152–161.

83. Thangadurai, V., Kaack, H., and Weppner, W.J.F. (2003). Novel fast lithium ion conduction in garnet-type $Li_5La_3M_2O_{12}$ (M = Nb, Ta). J. Am. Ceram. Soc. *86*, 437–440.

84. Awaka, J., Takashima, A., Kataoka, K., Kijima, N., Idemoto, Y., and Awaka, J. (2011). Crystal structure of fast lithium-ion-conducting cubic $Li_7La_3Zr_2O_{12}$. Chem. Lett. *40*, 60–62.

85. Awaka, J., Kijima, N., Hayakawa, H., and Akimoto, J. (2009). Synthesis and structure analysis of tetragonal $Li_7La_3Zr_2O_{12}$ with the garnet-related type structure. J. Solid State Chem. *182*, 2046–2052.

86. Stramare, S., Thangadurai, V., and Weppner, W. (2003). Lithium lanthanum titanates: a review. Chem. Mater. *15*, 3974–3990.

87. Li, Y., Han, J.T., Wang, C.A., Xie, H., and Goodenough, J.B. (2012). Optimizing Li^+ conductivity in a garnet framework. J. Mater. Chem. *22*, 15357–15361.

88. Allen, J.L., Wolfenstine, J., Rangasamy, E., and Sakamoto, J. (2012). Effect of substitution (Ta, Al, Ga) on the conductivity of $Li_7La_3Zr_2O_{12}$. J. Power Sources *206*, 315–319.

89. Ohta, S., Kobayashi, T., and Asaoka, T. (2011). High lithium ionic conductivity in the garnet-type oxide $Li_{7-X}La_3(Zr_{2-X}, Nb_X)O_{12}$ (X=0-2). J. Power Sources *196*, 3342–3345.

90. Deviannapoorani, C., Dhivya, L., Ramakumar, S., and Murugan, R. (2013). Lithium ion transport properties of high conductive tellurium substituted $Li_7La_3Zr_2O_{12}$ cubic lithium garnets. J. Power Sources *240*, 18–25.

91. Wu, J.F., Chen, E.Y., Yu, Y., Liu, L., Wu, Y., Pang, W.K., Peterson, V.K., and Guo, X. (2017). Gallium-doped $Li_7La_3Zr_2O_{12}$ garnet-type electrolytes with high lithium-ion conductivity. ACS Appl. Mater. Interfaces *9*, 1542–1552.

92. Li, Y.T., Xu, B.Y., Xu, H.H., Duan, H.N., Lu, X.J., Xin, S., Zhou, W.D., Xue, L.G., Fu, G.T., Manthiram, A., et al. (2017). Hybrid polymer/garnet electrolyte with a small interfacial resistance for lithium-ion batteries. Angew. Chem. Int. Ed. *56*, 753–756.

93. Itoh, M., Inaguma, Y., Jung, W.-H., Chen, L., and Nakamura, T. (1994). High lithium ion conductivity in the perovskite-type compounds $Ln_{12}Li_{12}TiO_3$(Ln=La,Pr,Nd,Sm). Solid State Ion. *70*, 203–207.

94. Zhao, Y., and Daemen, L.L. (2012). Superionic conductivity in lithium-rich anti-perovskites. J. Am. Chem. Soc. *134*, 15042–15047.

95. Abrahams, I., and Hadzifejzovic, E. (2000). Lithium ion conductivity and thermal behaviour of glasses and crystallised glasses in the system Li_2O-Al_2O_3-TiO_2-P_2O_5. Solid State Ion. *134*, 249–257.

96. West, A. (1975). Crystal chemistry of some tetrahedral oxides. Z. Kristallogr. Cryst. Mater. *141*, 422–436.

97. Murayama, M., Kanno, R., Irie, M., Ito, S., Hata, T., Sonoyama, N., and Kawamoto, Y. (2002). Synthesis of new lithium ionic conductor thio-LISICON—lithium silicon sulfides system. J. Solid State Chem. *168*, 140–148.

98. Mo, Y., Ong, S.P., and Ceder, G. (2012). First principles study of the $Li_{10}GeP_2S_{12}$ lithium super ionic conductor material. Chem. Mater. *24*, 15–17.

99. Wang, Y., Richards, W.D., Ong, S.P., Miara, L.J., Kim, J.C., Mo, Y., and Ceder, G. (2015). Design principles for solid-state lithium superionic conductors. Nat. Mater. *14*, 1026–1031.

100. Chen-Yang, Y.W., Chen, H.C., Lin, F.J., and Chen, C.C. (2002). Polyacrylonitrile electrolytes: 1. a novel high-conductivity composite polymer electrolyte based on PAN, $LiClO_4$ and α-Al_2O_3. Solid State Ion. *150*, 327–335.

101. Liu, Y., Lee, J.Y., and Hong, L. (2004). In situ preparation of poly(ethylene oxide)-SiO_2 composite polymer electrolytes. J. Power Sources *129*, 303–311.

102. Sun, H., Takeda, Y., Imanishi, N., Yamamoto, O., and Sohn, H.J. (2000). Ferroelectric materials as a ceramic filler in solid composite polyethylene oxide-based electrolytes. J. Electrochem. Soc. *147*, 2462–2467.

103. Liu, W., Lee, S.W., Lin, D., Shi, F., Wang, S., Sendek, A.D., and Cui, Y. (2017). Enhancing ionic conductivity in composite polymer electrolytes with well-aligned ceramic nanowires. Nat. Energy *2*, https://doi.org/10.1038/nenergy.2017.35.

104. Yang, T., Zheng, J., Cheng, Q., Hu, Y.-Y., and Chan, C.K. (2017). Composite polymer electrolytes with $Li_7La_3Zr_2O_{12}$ garnet-type nanowires as ceramic fillers: mechanism of conductivity enhancement and role of doping and morphology. ACS Appl. Mater. Interfaces *9*, 21773–21780.

105. He, Z., Chen, L., Zhang, B., Liu, Y., and Fan, L.Z. (2018). Flexible poly (ethylene carbonate)/garnet composite solid electrolyte reinforced by poly (vinylidene fluoride-hexafluoropropylene) for lithium metal batteries. J. Power Sources *392*, 232–238.

106. Kumar, B., Rodrigues, S.J., and Scanlon, L.G. (2001). Ionic conductivity of polymer-ceramic composites. J. Electrochem. Soc. *148*, A1191–A1195.

107. Marcinek, M., Bac, A., Lipka, P., Zalewska, A., Żukowska, G., Borkowska, R., and Wieczorek, W. (2000). Effect of filler surface group on ionic interactions in PEG-$LiClO_4$-Al_2O_3 composite polyether electrolytes. J. Phys. Chem. B *104*, 11088–11093.

108. Fu, K.K., Gong, Y., Dai, J., Gong, A., Han, X., Yao, Y., Wang, C., Wang, Y., Chen, Y., Yan, C., et al. (2016). Flexible, solid-state, ion-conducting membrane with 3D garnet nanofiber networks for lithium batteries. Proc. Natl. Acad. Sci. U S A. *113*, 7094–7099.

109. Lin, D., Yuen, P.Y., Liu, Y., Liu, W., Liu, N., Dauskardt, R.H., and Cui, Y. (2018). A silica-aerogel-reinforced composite polymer electrolyte with high ionic conductivity and high modulus. Adv. Mater. *30*, e1802661.

110. Liu, W., Lin, D., Sun, J., Zhou, G., and Cui, Y. (2016). Improved lithium ionic conductivity in composite polymer electrolytes with oxide-ion conducting nanowires. ACS Nano *10*, 11407–11413.

111. Zhai, H., Xu, P., Ning, M., Cheng, Q., Mandal, J., and Yang, Y. (2017). A flexible solid composite electrolyte with vertically aligned and connected ion-conducting nanoparticles for lithium batteries. Nano Lett. *17*, 3182–3187.

112. Li, D., Chen, L., Wang, T., and Fan, L.-Z. (2018). 3D Fiber-network-reinforced bicontinuous composite solid electrolyte for dendrite-free lithium metal batteries. ACS Appl. Mater. Interfaces *10*, 7069–7078.

113. Ruiz-Hitzky, E., and Aranda, P. (1990). Polymer-salt intercalation complexes in layer silicates. Adv. Mater. *2*, 545–547.

114. Lutkenhaus, J.L., Olivetti, E.A., Verploegen, E.A., Cord, B.M., Sadoway, D.R., and Hammond, P.T. (2007). Anisotropic structure and transport in self-assembled layered polymer-clay nanocomposites. Langmuir *23*, 8515–8521.

115. Vaia, R.A., Vasudevan, S., Krawiec, W., Scanlon, L.G., and Giannelis, E.P. (1995). New polymer electrolyte nanocomposites: melt intercalation of poly (ethylene oxide) in mica-type silicates. Adv. Mater. *7*, 154–156.

116. Wang, S., Shi, Q.X., Ye, Y.S., Wang, Y., Peng, H.Y., Xue, Z.G., Xie, X.L., and Mai, Y.W. (2017). Polymeric ionic liquid-functionalized mesoporous silica nanoplates: a new high-performance composite polymer electrolyte for lithium batteries. Electrochim. Acta *245*, 1010–1022.

117. Chen, L., Li, Y., Li, S.P., Fan, L.Z., Nan, C.W., and Goodenough, J.B. (2018). PEO/garnet composite electrolytes for solid-state lithium batteries: from "ceramic-in-polymer" to "polymer-in-ceramic". Nano Energy *46*, 176–184.

118. Zhang, X., Xie, J., Shi, F., Lin, D., Liu, Y., Liu, W., Pei, A., Gong, Y., Wang, H., Liu, K., et al. (2018). Vertically aligned and continuous nanoscale ceramic-polymer interfaces in composite solid polymer electrolytes for enhanced ionic conductivity. Nano Lett. *18*, 3829–3838.

119. Xiong, S., Liu, Z., Rong, H., Wang, H., McDaniel, M., and Chen, H. (2018). $Na_3SbSe_{4-x}S_x$ as sodium superionic conductors. Sci. Rep. *8*, 9146.

120. Lee, K., Kim, S., Park, J., Park, S.H., Coskun, A., Jung, D.S., Cho, W., and Choi, J.W. (2017). Selection of binder and solvent for solution-processed all-solid-state battery. J. Electrochem. Soc. *164*, A2075–A2081.

121. Li, W., Yao, H., Yan, K., Zheng, G., Liang, Z., Chiang, Y.M., and Cui, Y. (2015). The synergetic effect of lithium polysulfide and lithium nitrate to prevent lithium dendrite growth. Nat. Commun. *6*, 7436.

122. Monroe, C., and Newman, J. (2005). The impact of elastic deformation on deposition kinetics at lithium/polymer interfaces. J. Electrochem. Soc. *152*, A396–A404.

123. Ren, Y., Shen, Y., Lin, Y., and Nan, C.-W. (2015). Direct observation of lithium dendrites inside garnet-type lithium-ion solid electrolyte. Electrochem. Commun. *57*, 27–30.

124. Zhang, Z.H., Zhao, Y.R., Chen, S.J., Xie, D.J., Yao, X.Y., Cui, P., and Xu, X.X. (2017). An advanced construction strategy of all-solid-state lithium batteries with excellent interfacial compatibility and ultralong cycle life. J. Mater. Chem. A. *5*, 16984–16993.

125. Ban, X., Zhang, W., Chen, N., and Sun, C. (2018). A high-performance and durable poly (ethylene oxide)-based composite solid electrolyte for all solid-state lithium battery. J. Phys. Chem. C *122*, 9852–9858.

126. Sun, B., Mindemark, J., Edström, K., and Brandell, D. (2014). Polycarbonate-based solid polymer electrolytes for Li-ion batteries. Solid State Ion. *262*, 738–742.

127. Sheng, O., Jin, C., Luo, J., Yuan, H., Huang, H., Gan, Y., Zhang, J., Xia, Y., Liang, C., and Zhang, W. (2018). $Mg_2B_2O_5$ nanowire enabled multifunctional solid-state electrolytes with high ionic conductivity, excellent mechanical properties, and flame-retardant performance. Nano Lett. *18*, 3104–3112.

128. Koo, M., Park, K.I., Lee, S.H., Suh, M., Jeon, D.Y., Choi, J.W., Kang, K., and Lee, K.J. (2012). Bendable inorganic thin-film battery for fully flexible electronic systems. Nano Lett. *12*, 4810–4816.

129. Li, Y., Zhou, W., Xin, S., Li, S., Zhu, J., Lü, X., Cui, Z., Jia, Q., Zhou, J., Zhao, Y., et al. (2016). Fluorine-doped antiperovskite electrolyte for all-solid-state lithium-ion batteries. Angew. Chem. Int. Ed. *55*, 9965–9968.

130. Tao, Y.C., Chen, S.J., Liu, D., Peng, G., Yao, X.Y., and Xu, X.X. (2016). Lithium superionic conducting oxysulfide solid electrolyte with excellent stability against lithium metal for all-solid-state cells. J. Electrochem. Soc. *163*, A96–A101.

131. Zhu, Z., Hong, M., Guo, D., Shi, J., Tao, Z., and Chen, J. (2014). All-solid-state lithium organic battery with composite polymer electrolyte and pillar[5]quinone Cathode. J. Am. Chem. Soc. *136*, 16461–16464.

132. Van Den Broek, J., Afyon, S., and Rupp, J.L. (2016). Interface-engineered all-solid-state Li-ion batteries based on garnet-type fast Li^+ conductors. Adv. Energy Mater. *6*, 1600736.

133. Zhou, W., Wang, S., Li, Y., Xin, S., Manthiram, A., and Goodenough, J.B. (2016). Plating a dendrite-free lithium anode with a polymer/ceramic/polymer sandwich electrolyte. J. Am. Chem. Soc. *138*, 9385–9388.

134. Ohta, S., Seki, J., Yagi, Y., Kihira, Y., Tani, T., and Asaoka, T. (2014). Co-sinterable lithium garnet-type oxide electrolyte with cathode for all-solid-state lithium ion battery. J. Power Sources *265*, 40–44.

135. Wu, J.F., Pang, W.K., Peterson, V.K., Wei, L., and Guo, X. (2017). Garnet-type fast Li-ion conductors with high ionic conductivities for all-solid-state batteries. ACS Appl. Mater. Interfaces *9*, 12461–12468.

136. Li, Y., Chen, X., Dolocan, A., Cui, Z., Xin, S., Xue, L., Xu, H., Park, K., and Goodenough, J.B. (2018). Garnet electrolyte with an ultralow interfacial resistance for Li-metal batteries. J. Am. Chem. Soc. *140*, 6448–6455.

137. Liu, T., Zhang, Y., Zhang, X., Wang, L., Zhao, S.-X., Lin, Y.H., Shen, Y., Luo, J., Li, L., and Nan, C.W. (2018). Enhanced electrochemical performance of bulk type oxide ceramic lithium batteries enabled by interface modification. J. Mater. Chem. A *6*, 4649–4657.

138. Bruce, P.G., Freunberger, S.A., Hardwick, L.J., and Tarascon, J.M. (2012). Li-O_2 and Li-S batteries with high energy storage. Nat. Mater. *11*, 19–29.

139. Ji, X., Lee, K.T., and Nazar, L.F. (2009). A highly ordered nanostructured carbon-sulphur cathode for lithium-sulphur batteries. Nat. Mater. *8*, 500–506.

140. Marmorstein, D., Yu, T., Striebel, K., McLarnon, F., Hou, J., and Cairns, E. (2000). Electrochemical performance of lithium/sulfur cells with three different polymer electrolytes. J. Power Sources *89*, 219–226.

141. Hassoun, J., and Scrosati, B. (2010). Moving to a solid-state configuration: a valid approach to making lithium-sulfur batteries viable for practical applications. Adv. Mater. *22*, 5198–5201.

142. Liang, X., Wen, Z., Liu, Y., Zhang, H., Huang, L., and Jin, J. (2011). Highly dispersed sulfur in ordered mesoporous carbon sphere as a composite cathode for rechargeable polymer Li/S battery. J. Power Sources *196*, 3655–3658.

143. Lin, Y., Wang, X., Liu, J., and Miller, J.D. (2017). Natural halloysite nano-clay electrolyte for advanced all-solid-state lithium-sulfur batteries. Nano Energy *31*, 478–485.

144. Yamada, T., Ito, S., Omoda, R., Watanabe, T., Aihara, Y., Agostini, M., Ulissi, U., Hassoun, J., and Scrosati, B. (2015). All solid-state lithium-sulfur battery using a glass-type P_2S_5-Li_2S electrolyte: benefits on anode kinetics. J. Electrochem. Soc. *162*, A646–A651.

145. Yao, X., Huang, N., Han, F., Zhang, Q., Wan, H., Mwizerwa, J.P., Wang, C., and Xu, X. (2017). High-performance all-solid-state lithium-sulfur batteries enabled by amorphous sulfur-coated reduced graphene oxide cathodes. Adv. Energy Mater. *7*, 1602923.

146. Xu, R.C., Xia, X.H., Wang, X.L., Xia, Y., and Tu, J.P. (2017). Tailored Li_2S-P_2S_5 glass-ceramic electrolyte by MoS_2 doping, possessing high ionic conductivity for all-solid-state lithium-sulfur batteries. J. Mater. Chem. A *5*, 2829–2834.

147. Hassoun, J., Croce, F., Armand, M., and Scrosati, B. (2011). Investigation of the O_2 electrochemistry in a polymer electrolyte solid-state cell. Angew. Chem. Int. Ed. *123*, 3055–3058.

148. Kitaura, H., and Zhou, H.S. (2012). Electrochemical performance of solid-state lithium-air batteries using carbon nanotube catalyst in the air electrode. Adv. Energy Mater. *2*, 889–894.

149. Balaish, M., Peled, E., Golodnitsky, D., and Ein-Eli, Y. (2015). Liquid-free lithium-oxygen batteries. Angew. Chem. Int. Ed. *127*, 446–450.

150. Kitaura, H., and Zhou, H. (2012). Electrochemical performance and reaction mechanism of all-solid-state electrochemical performance and reaction mechanism of all-solid-state lithium-air batteries composed of lithium, $Li_{1+x}Al_yGe_{2-y}(PO_4)$ solid electrolyte and carbon nanotube air electrode. Energy Environ. Sci. *5*, 9077–9084.